การออกแบบและควบคุมหุ่นยนต์กายภาพบำบัดแบบสององศาอิสระพร้อมกิจกรรมบนสภาพแวดล้อมเสมือน

นายณัฐพงษ์ อังศุภศิริกุล

วิทยานิพนธ์นี้เป็นส่วนหนึ่งของการศึกษาตามหลักสูตรปริญญาวิศวกรรมศาสตรมหาบัณฑิต
สาขาวิชาวิศวกรรมเครื่องกล ภาควิชาวิศวกรรมเครื่องกล
คณะวิศวกรรมศาสตร์ จุฬาลงกรณ์มหาวิทยาลัย
ปีการศึกษา 2560

DESIGN AND CONTROL OF A 2-DOF REHABILITATION ROBOT WITH A TASK DEFINED IN A VIRTUAL EN VIRONMENT.

Mr. Natthapong Angsupasirikul

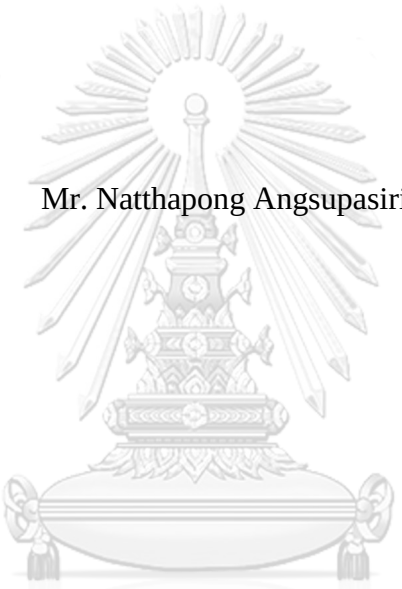

A Thesis Submitted in Partial Fulfillment of the Requirements
for the Degree of Master of Engineering Program in Mechanical Engineering
Department of Mechanical Engineering
Faculty of Engineering
Chulalongkorn University
Academic Year 2017

Thesis Title	DESIGN AND CONTROL OF A 2-DOF REHABILITATION ROBOT WITH A TASK DEFINED IN A VIRTUAL ENVIRONMENT.
By	Mr. Natthapong Angsupasirikul
Field of Study	Mechanical Engineering
Thesis Advisor	Associate Professor Ratchatin Chancharoen, Ph.D.

Accepted by the Faculty of Engineering, Chulalongkorn University in Partial Fulfillment of the Requirements for the Master's Degree

.....Dean of the Faculty of Engineering
(Associate Professor Supot Teachavorasinskun, D.Eng.)

THESIS COMMITTEE

.....Chairman
(Professor Viboon Sangveraphunsiri, Ph.D.)

.....Thesis Advisor
(Associate Professor Ratchatin Chancharoen, Ph.D.)

.....Examiner
(Gridsada Phanomchoeng, Ph.D.)

.....External Examiner
(Winai Chonnaparamutt, Ph.D.)

ณัฐพงษ์ อังศุภศิริกุล : การออกแบบและควบคุมหุ่นยนต์กายภาพบำบัดแบบสององศาอิสระพร้อมกิจกรรมบนสภาพแวดล้อมเสมือน (DESIGN AND CONTROL OF A 2-DOF REHABILITATION ROBOT WITH A TASK DEFINED IN A VIRTUAL ENVIRONMENT.) อ.ที่ปรึกษาวิทยานิพนธ์หลัก: รศ. ดร.รัชทิน จันทร์เจริญ, หน้า.

โครงการวิจัยนี้ได้นำเสนอระบบหุ่นยนต์กายภาพบำบัดแขน โดยมีลักษณะเป็นแบบปลายแขนกลสององศาอิสระ ซึ่งหุ่นยนต์ที่ออกแบบมีลักษณะกระทัดรัด ใช้งานง่าย และดูปลอดภัย ระบบหุ่นยนต์กายภาพบำบัดนี้ประกอบด้วยตัวหุ่นยนต์ ระบบควบคุม และสภาพแวดล้อมเสมือน (เกม) ระบบหุ่นยนต์กายภาพบำบัดนี้ได้ถูกทดสอบกับผู้ที่มีสุขภาพแข็งแรง 2 คน โดยมีการทดสอบในรูปแบบพาสซีฟ แบบแอคทีฟไม่มีการช่วยเหลือ และแบบแอคทีฟซึ่งมีการช่วยเหลือตามความตั้งใจ

ภาควิชา วิศวกรรมเครื่องกล ลายมือชื่อนิสิต .....

สาขาวิชา วิศวกรรมเครื่องกล ลายมือชื่อ อ.ที่ปรึกษาหลัก .....

ปีการศึกษา 2560

5770168321 : MAJOR MECHANICAL ENGINEERING
KEYWORDS: REHABILITATTION ROBOT / HAND AND ARM REHABILITATION

NATTHAPONG ANGSUPASIRIKUL: DESIGN AND CONTROL OF A 2-DOF REHABILITATION ROBOT WITH A TASK DEFINED IN A VIRTUAL ENVIRONMENT.. ADVISOR: ASSOC. PROF. RATCHATIN CHANCHAROEN, Ph.D., pp.

This research proposes a novel upper-limb rehabilitation robotic system. Instead of an exoskeleton type, the proposed robot is designed as active 2-DOF end-effector type moving in a horizontal plane, with being compact and easy to use with the harmless image. The rehabilitation robot system consists of a robot, a controller system and a virtual environment (game). The proposed rehabilitation robot system has been evaluated with 2 healthy subjects. The robot system has been evaluated in passive, active non-assist and active intent-based assistive rehabilitation type.

Department: Mechanical Engineering Student's Signature .....
Field of Study: Mechanical Engineering Advisor's Signature .....
Academic Year: 2017

ACKNOWLEDGEMENTS

Firstly, the author would like to thank Assoc. Prof. Ratchatin Chancharoen for being an advisor for years in Master of Engineering. He has given many advises regarding studying, researching, and conducting this thesis. He also gave many advises in non study related matters. Secondly, thanks to my friends for being tested subjects even it took a long time. Lastly, thanks to my family for giving supports in many ways through this research.

CONTENTS

Page

Page

LIST OF TABLES

LIST OF FIGURES

LIST OF EQUATIONS

CHAPTER 1
INTRODUCTION

1.1 Statement of Problem

Recently, Number of stroke patients is increasing. The common outcomes of stroke are Hemiparesis or Hemiplegia [1]. After a stroke patient has been cured, the post-stroke patient requires intense and efficient rehabilitation to recover motor function [2]. Rehabilitation robotics has drawn attention from researchers all over the world as conventional rehabilitation by a therapist is time-consuming and expensive. With a rehabilitation robot, the patient can exercise more frequently resulting in faster recovery.

A Virtual Environment is needed to efficiently rehabilitate with the robot, especially in active rehabilitation, since it can provide interesting tasks to the patients and keep them motivated [3].

1.2 Objective

1. To study rehabilitation robot designing.

2. To design and develop an upper-limb rehabilitation robot with virtual environment system, for passive and active rehabilitation of post-stroke patients.

1.3 Research Scope

Design and construct a rehabilitation robot system, including

1. Robot (Mechanical hardware).
2. Electronics (Electrical hardware).
3. Controller (Controller software).
4. Virtual Environment (Software).

1.4 Approach

1. Literature reviewing of rehabilitation robots.
2. Conceptual design of a rehabilitation robot system.
3. Design and build a prototype of a rehabilitation robot (Hardware).
4. Design electronics and controller system for built rehabilitation robot.
5. Design a virtual environment for rehabilitation
6. Evaluate the prototype system.
7. Analyze the prototype system for improvement.
8. Design and build the second prototype of the rehabilitation robot (Hardware).
9. Improve the controller system and the virtual environment.
10. Evaluate the second prototype.
11. Analyze data and conclusion.

1.5 Benefits

1. Understanding in upper limb rehabilitation.

2. A prototype of a rehabilitation robot system which can be improved into a commercial product in the future.

3. Techniques in collaborative robot controlling.

CHAPTER 2
LITERATURE REVIEW

2.1 Theoretical Background

2.1.1 Post-Stroke Rehabilitation

After a stroke patient has been cured, the post-stroke patient will continue experiencing movement impairment. This movement impairment is categorized into 6-stage Brunnstrom [4].

Table 2.1 6-Stages Brunnstrom recovery of the post-stroke patients.

	Stages	Definition
1	Flaccidity	The patient is not able to initiate muscle movement of the affected side. Active rehabilitation is not possible.
2	Spasticity occurs	The patient's limb resists to some passive motion. The patient's limb is usually at a static pose.
3	Increased spasticity	The spasticity is increased to the peak. The patient may able to initiate movement, but still unable to control.
4	Decreased spasticity	The spasticity is decreasing. The patient is starting to regain movement control.
5	Coordination is recovering	The spasticity is decreasing, and coordination of muscle is improved. Complex voluntary movement is possible.
6	Spasticity disappears.	The spasticity disappears completely. The patient regains the most of control.

During the first three stages, the patient needs passive rehabilitation to maintain and increase Range of Motion (ROM). After the patient can initiate movement, active rehabilitation is needed to recover motor function.

Many rehabilitation methods have been proposed in the past, but all of them belong to either passive or active rehabilitation. Active rehabilitation methods can be categorized into more groups.

Passive rehabilitation is the simplest rehabilitation. Passive rehabilitation can be done by either a therapist or a robot. In passive rehabilitation, the patient's limb movement is controlled by the rehabilitation provider. The purpose of passive rehabilitation is to maintain and increase ROM of the patient. The passive rehabilitation can be done in the patients at every Brunnstrom recovery stages. The MIME [5] (Mirror Image Movement Enabler) rehabilitation method is also a passive rehabilitation. The MIME method is to let the patient control the weakened limb by controlling the robot with the functional limb.

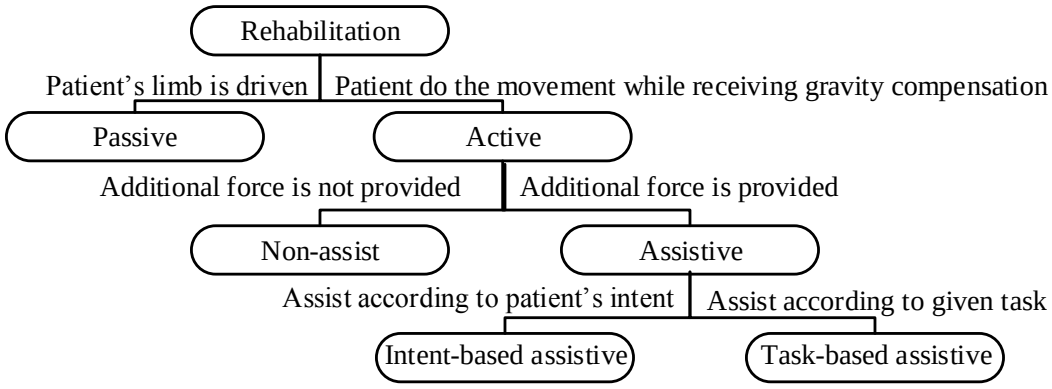

Figure 2.1 Types of rehabilitation.

During the third Brunnstrom stage, the patient is able to initiate motion. At this stage, active rehabilitation is needed to train motor function. In active rehabilitation, the patient's limb motion is initiated by the patient's intention while the robot is providing gravity compensation. Active rehabilitations which do not have assistive forces other than gravity compensation are called active non-assist rehabilitation, while the others are called active assistive rehabilitation.

There are two types of gravity compensation, passive and active. Passive gravity compensations are done without using actuators and control algorithms. Three techniques in providing passive gravity compensations are bearing support, spring force balancing and deadweight balancing. Bearing support is a technique which using bearing to disable movement along the gravity field. Spring force and deadweight balancing are techniques which store gravitational potential energy in springs and deadweights respectively.

In active assistive rehabilitation, there are additional assistive/resistive forces provided to the patient other than gravity compensation. Active rehabilitations with resistive forces are also included in active assistive rehabilitation. The assistive forces are either intent or task-based.

In intent based assistive/resistive active rehabilitation, the robot provides additional force according to the patient's intention. There are many ways to measure a patient's intention. F/T (Force/Torque) and sEMG (surface Electromyography) sensors are often used to observe the patient's intention. The F/T sensors detect the patient's intention by measuring contact force between the robot and the patient. The sEMG sensors detect the patient's intention by measuring the electric voltage of the patient skin generated by the underneath muscles. In task-based assistive/resistive active rehabilitation, the robot provides additional force according to the given task.

2.1.2 Human Anatomy

The human's upper-limb joints consist of rolling pieces of bones [6]. This makes human's joint very complex and difficult to be modeled. Rotation axes of the human joints usually move during motion [6]. The Misalignments between the human's joint axes and the robot joint axes create large reactional forces between the human's limb and the robot [7].

Many human upper-limb joint models have been proposed. One of them is a 9-DOF model [7] which consist of 2-DOF sternoclavicular, 3-DOF Glenohumeral (also known as shoulder ball joint), 1-DOF Elbow and 3-DOF Wrist joints. The shoulder ball joint is usually modeled as Ball and Socket joint. Many upper-limb exoskeleton designs, such as [8], use only 7-DOF by neglecting the Sternoclavicular joint. Since the exact locations of the human's joints are unknown, some rehabilitation robots are designed as end-effector robot. The end-effector robot is able to work without knowing the exact location of the human's joints. Another approach in eliminating the misalignment effects is adding an extra active or passive DOF [7].

In this research, the human's upper limb is modeled as 5-DOF in Figure 2.2. This 5-DOF human's upper-limb joints model consists of 3-DOF Shoulder joint, 1-DOF Elbow joint and 1-DOF Forearm joint. The 3-DOF Shoulder joint is modeled as Ball and Socket joint. The shoulder rotation axes are modeled as movement actions in Figure 2.3. ROMs of human's upper limb are also measured as minimum and maximum range of these movement actions.

The human's muscles configuration is very complex. Each of movement actions usually requires more than one muscles. Some muscles are responsible for more than one movement actions. The primary muscles for each movement actions are listed in Table 2.2.

Table 2.2 Primary muscles for actions

Action	Joint	Primary Muscles [9]
Horizontal Flexion	Shoulder	Pectoralis major, Deltoid anterior
Horizontal Extension	Shoulder	Latissimus dorsi, Deltoid posterior
Vertical Flexion	Shoulder	Pectoralis major, Deltoid anterior
Vertical Extension	Shoulder	Latissimus dorsi, Teres major
Adduction	Shoulder	Pectoralis major, Latissimus dorsi
Abduction	Shoulder	Deltoid all, Supraspinatus
Elbow Flexion	Elbow	Biceps brachii
Elbow Extension	Elbow	Triceps brachii

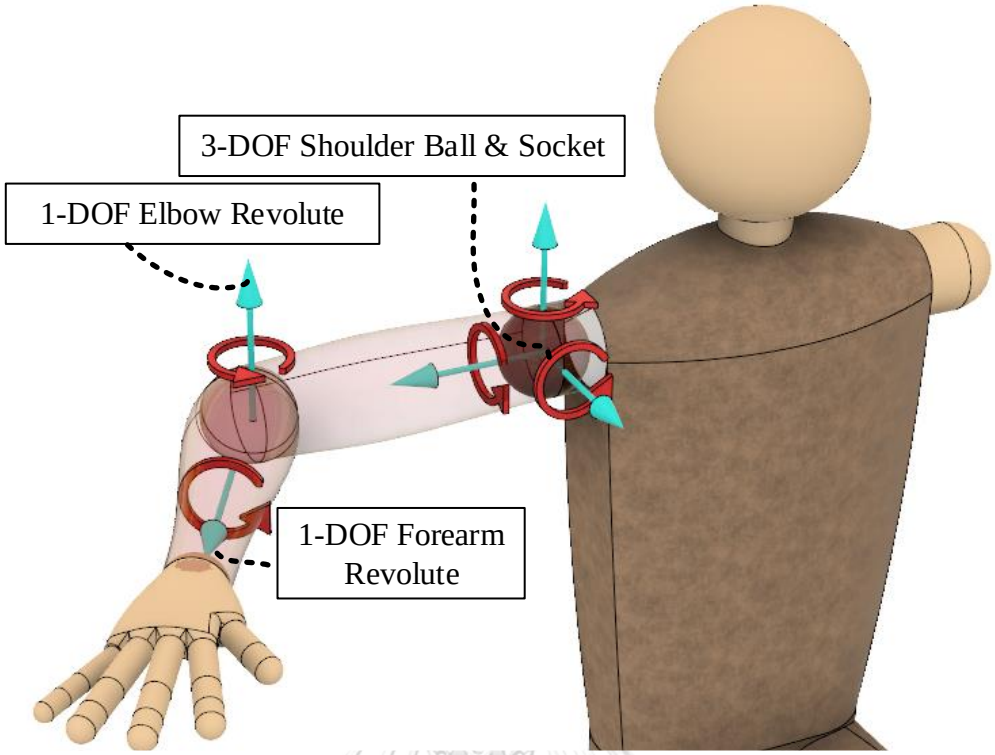

Figure 2.2 5-DOF human's upper-limb joints model.

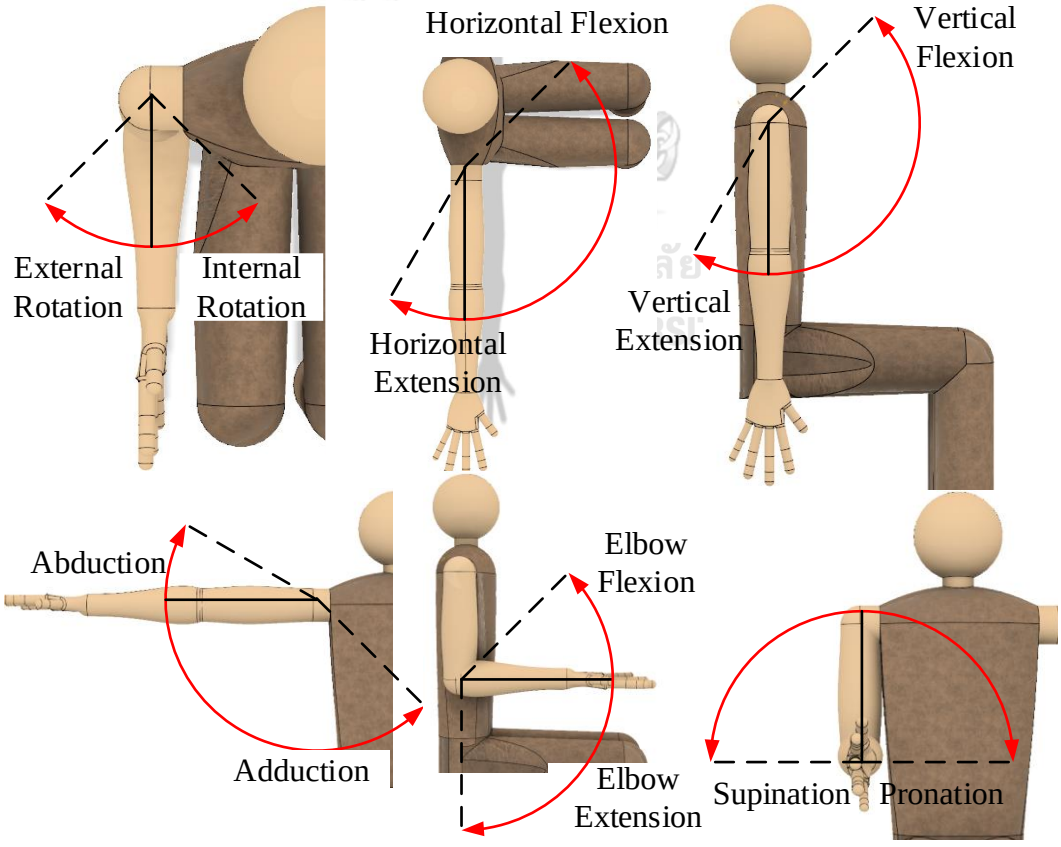

Figure 2.3 Upper-limb movement actions.

2.1.3 Rehabilitation Robots

There are two types of rehabilitation robots [1], which are end-effector and exoskeleton based robots. The end-effector based robots are usually simpler as it attaches to the patient's limb at only one point. The exoskeletons are usually designed as anthropomorphic which mapped its joints to the patient's joints. An exoskeleton must have adjustable mechanisms or extra joints to match with the patient's limb.

Rehabilitation robots are a type of cobots (collaborative robot). Every collaborative robot must be designed with safety concerns. The collaborative robots are usually able to sense interaction force. The interaction force between the human and the robot can be measured by a F/T sensor. Without a F/T sensor, a backdrivable transmissions are needed to observe interaction force at the actuators. The collaborative robots can assist the human in many ways, such as implementing a Virtual Wall in [10].

2.1.4 Virtual Environment

For active rehabilitation, a VE is needed for providing tasks to the patient and keeping the patient motivated. The VE can be either an activity or game-based. In activity-based VE, the mission is related to ADL (Activities of daily living) such as cooking.

Three types of tasks for rehabilitation are reaching, trajectory movement and free movement tasks.

Reaching tasks are the simplest and the most used tasks for rehabilitation. The objective is to move from one pose to another pose. An example of reaching tasks is pick and place task.

Trajectory movement tasks require the patient's limb to move along a given trajectory while staying inside acceptable distance from the trajectory. The given trajectory may be a straight or curved line, and the trajectory may lie in multidimensional space. Trajectory movement task can be described as in series continuous multiple reaching tasks.

Free movement tasks require the patient's limb to move and cover a surface, or a volume

2.2 Review of Previous works

There are many rehabilitation robots built in the past. Some interesting and well-known robots are chosen. The review will cover mechanical hardware, controllers, and virtual environment.

2.2.1 Mechanical Hardware Review

The reviewed rehabilitation robots are presented in Table 2.3. An industrial robot, such as PUMA 560 [5], is used in some experiment. In most rehabilitation robots, the exoskeleton-based design is preferred as it can directly manipulate human joints. Exoskeletons usually need 2 points of contact interface. The first robot is designed as a 2-DOF exoskeleton and only contact human hand at the handle. This makes the definition of the robot blurred and can be classified as end-effector as well.

Most of the rehabilitation robots use electric motors as actuators since they provide fast dynamic, torque control and may provide high backdrivability if use with backdrivable transmissions. For NEUROExos, hydraulic actuators are used to drive position of the tendon-driven compliant transmission, which results in force control of the robot joint. DC motors, both brushed and brushless, are used in most cases as it provides easy control, lightweight and very fast response. Some robots, such as CADEN-7, coreless brushed motors are used. Coreless brushed motors provide a high power-to-weight ratio, lightweight, low inertia and very fast response due to absent of iron core. However, for motors those require high torque and need not to be lightweight, AC motors are mostly chosen instead.

Safety is the most concerned topic in designing a robot to work with a human. For rehabilitation robotics, the most concerned topics are backdrivability of transmission and contact interface. Backdrivability is usually concerned when there is a chance that the robot can move the human's limb out of his/her reachable space. Mostly, rehabilitation robots use cable drive transmission which has high backdrivability, given that reduction ratio is not too high. MEDARM, Planar MEDARM, and CADEN-7 use cable drive transmission which sends power from the stationary motor through the other joints. For CADEN-7, cable transmissions are designed as long distance close-ended, which is very difficult to design as it needs to maintain the cable length when the other joints move. But in MEDARM and Planar MEDARM cases, these robots use open-ended by having redundant cable (actuators more than driven joints). The open-ended cable transmission does not require to maintain cable length (decreasing complexity and require less roller), but every joints actuation will be coupled. The another most safety transmission is damper transmission used in ATD. The damper transmission torque is proportional to slip velocity. For NEUROExos, hydraulic actuators are used. But these hydraulic send power through impedance (spring) controlled Bowden cable. With impedance-controlled Bowden cable transmission, the position of hydraulic is related with the joint torque. This technique makes the transmission become spring-like backdrivable.

Contact interface between human and robot also matters in safety concerns. In case that there is a fault, by program errors or other accident, the robot might move human's limb out of moving space and does damages. This safety concerns can be avoided by using an opened interface. With an opened interface, the user is free to remove his/her limb from the robot at will. The Planar MEDARM, which use only armrest instead of a cuff, is an example of an opened interface. Not only for safety concern but an opened interface will give user rest assured mind as well.

Table 2.3 Rehabilitation robots review

No.	Robot/Project Name [Reference]	Year	Type	Actuator	Transmission	DOF (Active/ Passive)	Interface (U-Upper Arm F-Forearm H-hand)	Passive Gravity Compensate
1.	N/A [11]	2001	Exoskeleton	Brushed DC Motors	Planetary	2/0	1-Handle-Opened	No
2.	PUMA 560 [5]	2002	End-Effector	Motors	N/A	6/0	1-H-Closed	No
3.	T-WREX [12]	2006	Exoskeleton	No actuator	No transmission	0/5	2-UF-Closed	Spring
4.	MEDARM [13]	2007		Motors	Open-ended Cable/Belt	6/0	2-UF-Closed	No
5.	Planar MEDARM [14]	2007		Motors	Open-ended Cable	3/0	3-UFH-Opened	Bearing
6.	CADEN-7 [8]	2007		Brushed DC Motors	Close-ended Cable	7/0	2-UF Closed/ 1-H Opened	No
7.	SUEFUL-7 [15]	2009		DC Motors	Pulley Cable/Gear	7/0	3-UFH-Closed	No
8.	MARSE-4 [16]	2011		Brushless DC Motors	Harmonic Drive + Gear	4/0	3-FH-Closed	No
9.	NEUROExos [17, 18]	2011		Hydraulic	Bowden Cable	1/4	2-UF-Closed	Spring
10.	CAREX [6, 19]	2012		AC Motors	Pulling Cable	5/0	2-UF-Closed	No
11.	ATD [20]	2014	End-Effector	DC Motors	Planetary Gear + Damper	3/0	1-F-Closed	Spring
12.	1st proposed prototype [21]	2015		Brushed DC Motors	Close-ended Cable	2/1	1-F-Opened	Bearing
13.	CUREs [22]	2017	Exoskeleton	Brushless DC Motors	Close-ended Cable	4/0	2-UF-Closed	Deadweight

2.2.2 Rehabilitation Controllers Review

The review of controllers used in rehabilitation robots are presented in Table 2.4. Of all rehabilitation operations, passive rehabilitation is the simplest since a simple PID can be used to control the robot. Almost all robots should be able to operate in passive rehabilitation. The MIME [5], Mirror Image Movement Enabler, is also classified as passive rehabilitation. Usually, backdrivability of the robot is required to operate in active rehabilitation. But the 2nd example, which uses PUMA 560, operate by using force feedback to apply force control.

To operate a rehabilitation robot in Intent based active assistive, either F/T or sEMG are needed. A simple proportional sEMG controller can be used to assist the elbow joint since the elbow joint is controlled by only 2 primary muscles. The 2 primary muscles for the elbow joint are Biceps and Triceps, acting in agonist/antagonist. For the other joints, many muscle signals are required. To control the other joints, a complex controller such as Neurofuzzy is needed to predict intention. Intent-based assistive using F/T sensors are simpler for utilization, as the sensor only attached to interfaces.

Task-based assistive controllers are simpler to implement. F/T and sEMG sensors are not necessary but still recommended. Assist-as-needed (AaN) is a concept to let the user do the task and assist when the user seems to fail in doing the task. The definition of failing is very indistinct, and many researches implemented this concept in many ways. The implemented AaN controllers in [22] is a passive rehabilitation controller with non-linear impedance applying very low driving force in case of low error (the user is doing the task) and apply exponentially strong driving force in case of higher position error from trajectory (the user is failing).

Table 2.4 Rehabilitation controllers review

No.	Rehabilitation Type	Controller Concept	Method / Note	Implemented Robot	Primary Signal (Position Sensor Excluded)
1	Passive	Position Control [5, 16, 20]	N/A	PUMA 560	F/T
			PID	MARSE-4	-
			PD over force control	ATD	F/T
		MIME [5]	Control by healthy limb	PUMA 560	F/T
2	Active Non-assist	No Controller [12]	Non-powered gravity support	T-WREX	-
		Powered Gravity Support [20]	PI Force Control	ATD	F/T
		Active Non-assist without gravity support [5]	No gravity support, impedance control on positioning.	PUMA 560	F/T
3	Intent Based Assistive	Force Amplifier [11]	sEMG Agonist/Antagonist with Force feedback	N/A	2-sEMG + F/T
		Active Resist [5]	Impedance control on positioning	PUMA 560	F/T
		Proportional EMG [23]	Processed sEMG	NEUROExos	2-sEMG
		sEMG Neurofuzzy [24]	16 Channel sEMG Neurofuzzy	SUEFUL-7	16-sEMG
		sEMG Classifier [25]	Extension/Flexion Classification	5-DOF Exoskeleton [26]	2-sEMG
4	Task Based Assistive	Force-Field Controller [6]	Force-Field Tunnel with Deadband	CAREX	Cable Tension (Load cell)
		Virtual Table Support [20]	PI Force Control	ATD	F/T
		Assist-as-needed [22]	Impedance Control	CUREs	-

2.2.3 Rehabilitation Tasks and Virtual Environments Review

In active rehabilitation, the patient is needed to be provided with tasks since the robot and the patient's limb are moved by the patient's intent. However, active rehabilitation using robot can be done in reality as in [6], but preparing a stage for rehabilitation is labor works and the tasks are monotonous. Utilizing VE in rehabilitation will increase in repetition, motivation and focused on training [27]. The review of rehabilitation tasks and virtual environments are shown in Table 2.5.

Table 2.5 Rehabilitation tasks and environments review

No.	Task Type	Activity/Game	Robot	Environment Type
1	Reaching	Shopping	T-WREX [12]	2D Activity Based
		Cracking Eggs		
		Washing the Arm		VE Mixed Reality
		Eating		
		Bug Hunt	Trackhold [27]	2D Activity Based
		Grab 2D		3D Activity Based
		Grab 3D		
		Bells (Ring a bell)	BRANDO [28]	3D Game-Based
		Balloons (Popping balloons)		
2	Trajectory	Follow circular path	CAREX [6]	Reality Game Based
		Block inserting		
		Twirl (Moving in a circle)	Trackhold [27]	2D Game-Based
3	Free	Sponge (Wiping screen)		
		Washing the Stove	T-WREX [12]	2D Activity Based

CHAPTER 3
DESIGN, CONSTRUCTION, AND CONTROL OF UPPER-LIMB REHABILITATION ROBOT

3.1 Hardware Design

3.1.1 Design Requirements

In designing a rehabilitation robot, safety is the most concerned topic. For safeness of utilizing the robot, the contact between human and robot should be an opened contact interface so that the user can pull his/her limb out in case of emergency. The proposed robot should meet with requirements:

1. The interface between robot and human must be an opened contact, which the user can pull his/her limb out at any time.
2. Mechanical working space of the robot should lie inside user motion ranges all the time.
3. The robot must be able to operate in both passive and active rehabilitation.
4. The robot should be able to provide at least one motion in Figure 2.3.
5. The robot actuator system should not be strong enough to damage human in any case.
6. The robot must have passive gravity compensation.
7. The robot must have high backdrivability transmission.

3.1.2 Kinematic Configuration Design

Because robot must have passive gravity compensation, the safest way to do is disable movements in the vertical direction with bearing support. The robot can be either an exoskeleton or end-effector based. An example of an exoskeleton configuration that fits the requirements is Planar MEDARM [14]. But an end-effector based have advantages that the robot can be easily used with any user without adjustment. Because the robot cannot move in a vertical direction and the interface must be an opened contact, a 2-DOF end-effector based robot which only moves in the horizontal plane is chosen. This design aims for operate in horizontal flexion/extension and elbow flexion/extension motions. Because some muscles for horizontal flexion/extension are also a part of abduction/adduction and vertical flexion/extension muscles, active rehabilitation of this motion may indirectly help in regaining all shoulder motion strength.

There are many kinematic configurations of robots that operate in the horizontal plane. The robot can be a two-link serial, a four-link closed chain or a Cartesian. A 2-DOF Prismatic Revolute manipulator configuration is chosen, since it is compact and resemble human workspace.

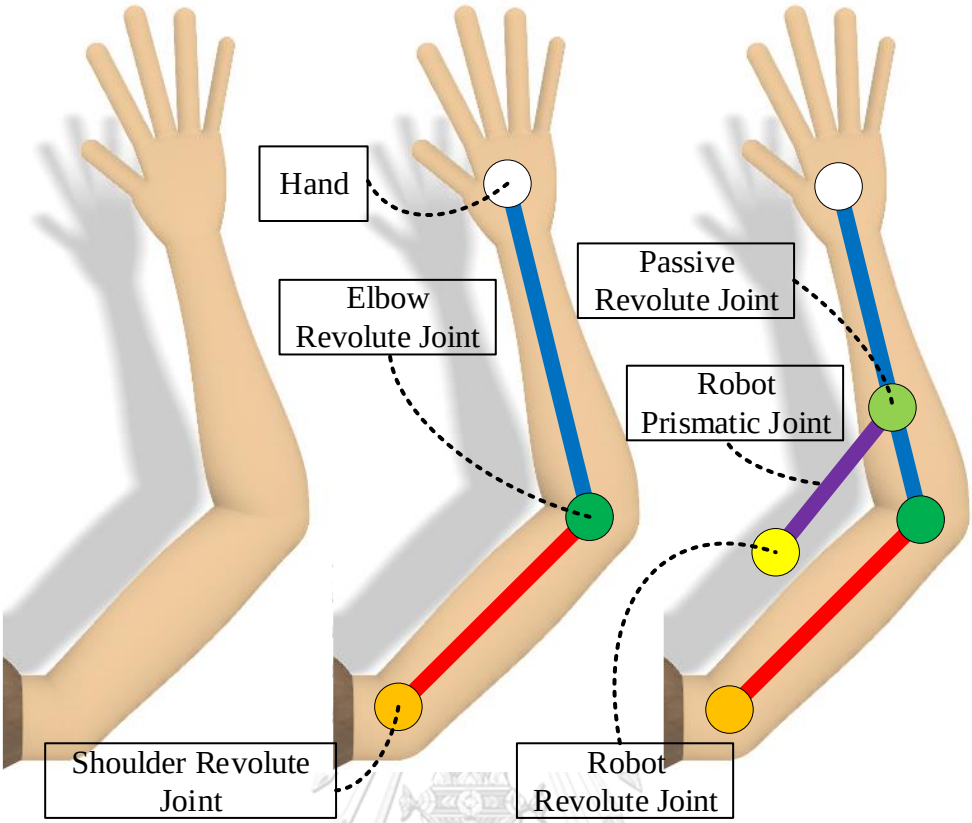

Figure 3.1 Kinematic of upper-limb and robot in the horizontal plane.

Figure 3.1 shows kinematic of human's upper-limb when moving in a horizontal plane at pose for horizontal flexion and extension. Movement of the limb can be mapped into a 2-DOF serial revolute joints manipulator. Because human's joints are not ideal revolute joint and their CR (center of rotation) keeps changing, the robot's kinematic must be designed to match these characteristics.

A 2-DOF Revolute-Prismatic, with an extra passive revolute joint beneath an end-effector, is proposed. This robot configuration can be mapped with a human's motion completely. There is no need to adjust the robot to match with the patient's arm length. With this configuration, it is possible to design an opened contact interface, by placing the patient's forearm on an end-effector.

Because the robot will be designed for horizontal flexion/extension and elbow flexion/extension, from this point onwards, 3-DOF shoulder ball joint is mapped as a 1-DOF revolute shoulder joint.

Table 3.1 Hardware Design Specification

Type	End-effector
Kinematic Configuration	2 DOF Revolute-Prismatic with 1 extra passive revolute joint
DOF (Active/Passive)	2/1
Passive Gravity Compensation	Bearing support
Human Machine Interface	Open Contact
Transmission	Closed-loop cable drive

3.1.3 First Prototype Design – Proof of Concept

The first prototype of a rehabilitation robot is designed according to hardware specification in Table 3.1. There are two Brushed DC motors as actuators, using cable transmission to reduces backlash and gives high back-drivability. Both motors have a rotary encoder attached at their rear and are used as position feedback. The motors are stationed to the base, so the inertia is very low. The second motor, controlling prismatic motion, transmits its power via a transmission shaft lies inside revolute joint while the motor itself is stationary. A linear guide is used as a prismatic joint, with linear block mounted to the robot 1st link (revolute joint) and linear rail act as robot 2nd link. The cable is tied from one end of the rail, winding around cable pinion and then tied at another end of the linear rail. This technique of cable transmission imitates rack and pinion configuration. This type of transmission is also used in [10], giving extraordinary high backdrivability. The end-effector is an opened armrest, with a revolute passive joint and a 6-axis F/T sensor attached below. If the user feels unsafe, he/she can pull his/her arm out. Figure 3.4 shows the robot while operating. Note that the design is to be used with a pose for horizontal flexion/extension (as in Figure 3.1), but It can also be used with partial vertical flexion (and shoulder abduction) pose. At partial vertical flexion pose, the motion of the shoulder is a mixed between vertical flexion/extension, horizontal flexion/extension, and abduction/abduction. The first prototype implementation has been written in [21].

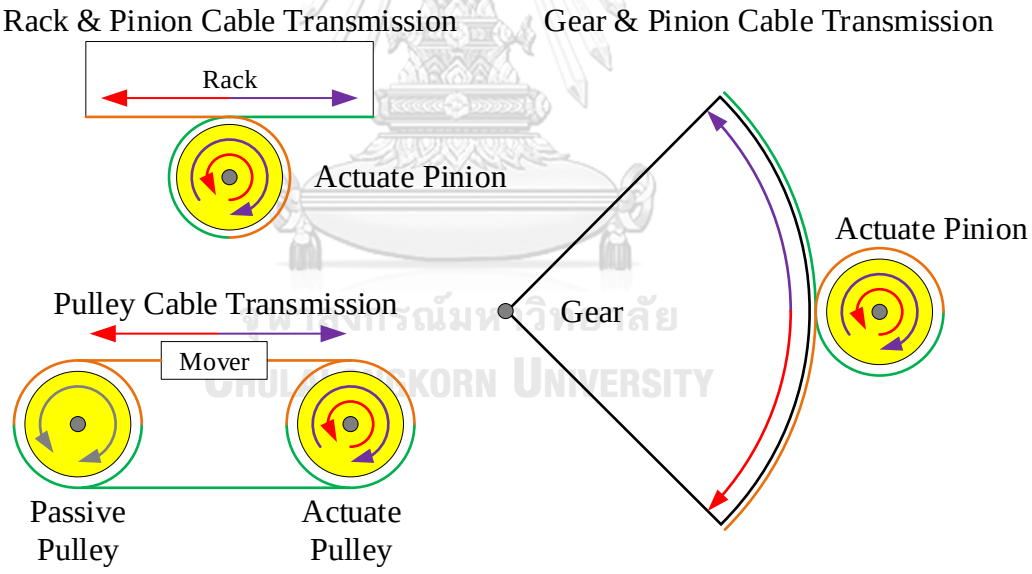

Figure 3.2 Cable transmission types

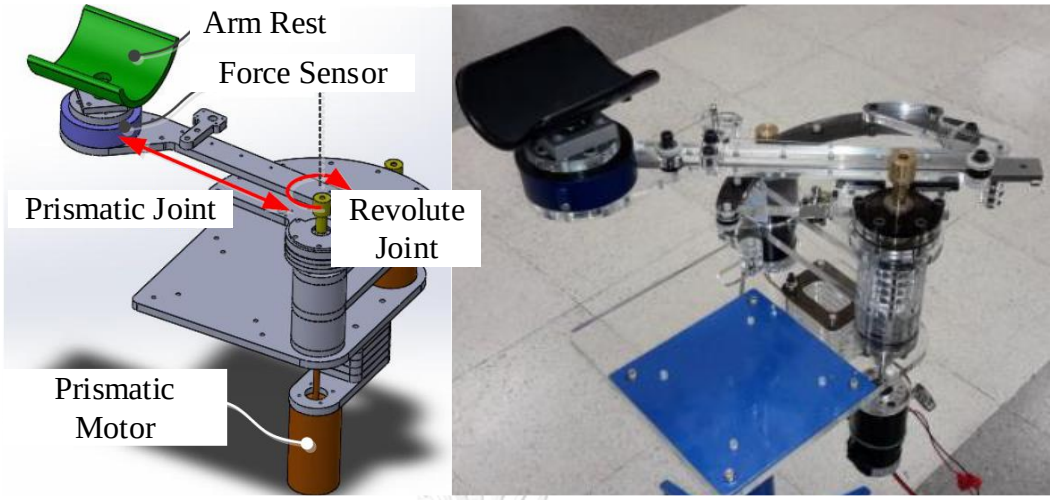

Figure 3.3 The first prototype, CAD (left), built model (right).

Figure 3.4 Utilization of the first prototype at partial vertical flexion pose

3.1.4 The Second Prototype Design

The first prototype is for proving of concept. To complete the research, the robot is redesigned with three major changes.

1. The motor controlling the prismatic joint will be moved from the base into the revolute joint bearing. Mounting the motor on the revolute link along with revolute joint axis will increase in revolute joint inertia only a little but removing transmission axis will drastically decrease prismatic joint friction and remove coupling effects.
2. Change prismatic cable drive transmission from rack and pinion into closed-loop pulley configuration. This change makes the friction increased as the tension is increased. But the advantage is that the moving part is smaller and lighter.

3. Make the robot compact and portable by design it to be installable to any table.

To make the robot lightweight and portable, all non-standard parts except cable drive pinions are designed to be manufactured by FDM 3D printer. The material is ABS. The design constraint is both motors are coreless brushed DC motor, with 35 mm diameter and 70 mm length (not include encoder), The chosen motors minimize system inertia, friction, and highest torque.

Because the second motor must lie inside the first joint bearing, and this bearing must withstand high moment as the end-effector move away from the revolute joint axis. A double row angular contact ball bearing with an inner diameter of 50 mm is chosen as the first joint bearing.

Table 3.2 Standard parts used in the second prototype design.

Type	Part Number	Description
1st joint revolute bearing	3210ATN9	Double row angular contact ball bearings, ID/OD = 50/90 mm
2nd joint linear guide	LWLF18-B	Linear guide, 240 mm
Bearing for cable drive pulley	F686A-ZZ	Ball bearing with a flanged outer ring, ID/OD = 6/13 mm
Passive joint bearing	3203ATN9	Double row angular contact ball bearings, ID/OD = 17/40 mm
1st and 2nd actuators	N/A	Maxon Coreless Brushed Motor, Diameter 35mm, Length 70mm
1st and 2nd position sensors	AEDM-5810-Z12	Incremental encoders, 5,000PPR (20,000 counts with quadrature decoder), attached at the motor rear.
Stainless sling for cable drive	N/A	0.8 mm diameter

3.1.4.1 Cable Drive Transmission Design

For the revolute joint, the cable drive transmission is designed as pinion-gear. The gear, which is the revolute link, is designed as a smooth arc of 120 degrees. The pinion is threaded. Reduction ratio to be chosen is a trade-off between backdrivability, position resolution, required torque and transmission thickness. The smallest pinion size is a constraint for choosing a reduction ratio. Too small pinion size leads to high stress of the stainless cable sling. Chosen pinion size is M14x1 thread. After optimization, the gear arc radius is 63.6 mm and the gear radius is 64 mm. This gives roughly a reduction ratio of 64:7. The exact reduction ratio is to be measured after manufacturing.

For the prismatic joint, cable drive is designed as closed-loop pulleys. Both active and passive pulleys are an M14x1 thread.

3.1.4.2 Robot Base Design

The base of the second's prototype role is

1. Mounting itself to a table
2. Mounting the 1st joint bearing at outer ring.
3. Mounting the 1st joint motor.

The robot base is designed as three parts to be assembled together. The 1st motor is mounted inside the Main Base, shifted from bearing axis according to a chosen reduction ratio. The Table Mount part is designed to be changeable without changing the Main Base in case it is not fit with some table. The Bearing Lock part is designed to press the bearing into the Main Base.

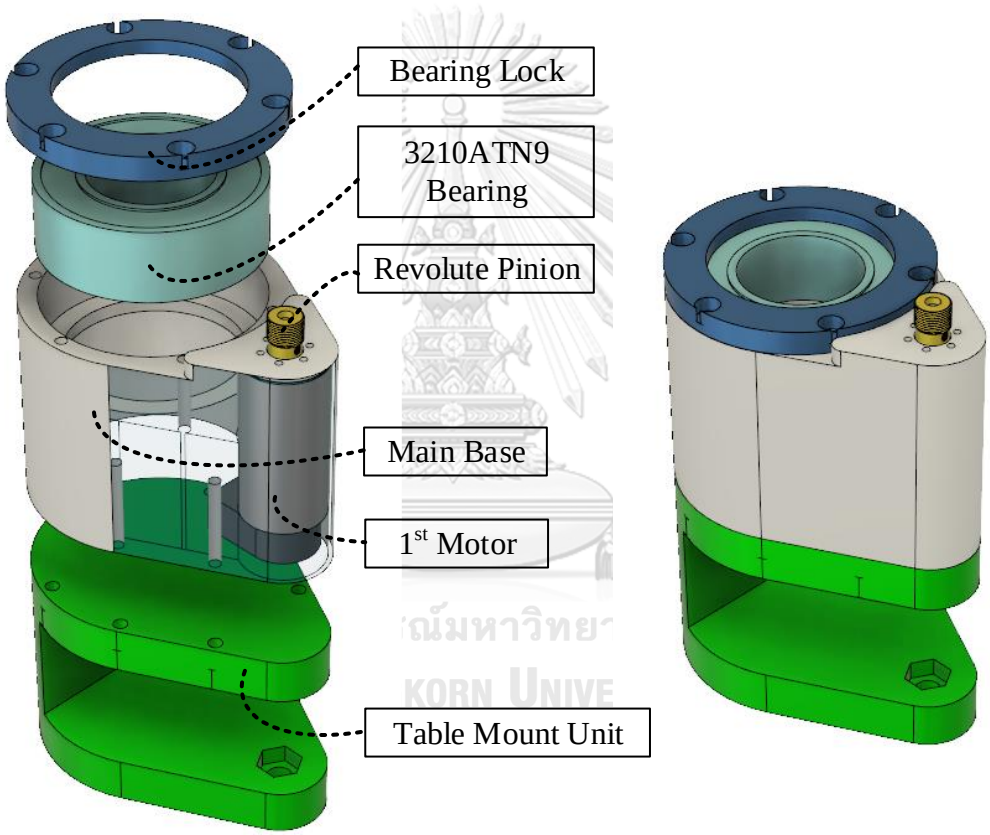

Figure 3.5 Robot base design

3.1.4.3 Revolute Joint Design

The role of the Revolute joint link is

1. A part of pinion-gear cable drive transmission, act as a gear.
2. Mounting the 2nd motor, coaxially with the 1st joint.
3. Mounting the linear rail for the prismatic joint.

The revolute joint is designed as three parts, having Revolute Link as the main part.

The Bearing Locker 1 and 2 are only for binding Revolute Link with the inner bearing. The Revolute Link has an arc to act as cable drive gear. It also has mechanical stoppers to limit the rotation between 0 and 135 degrees.

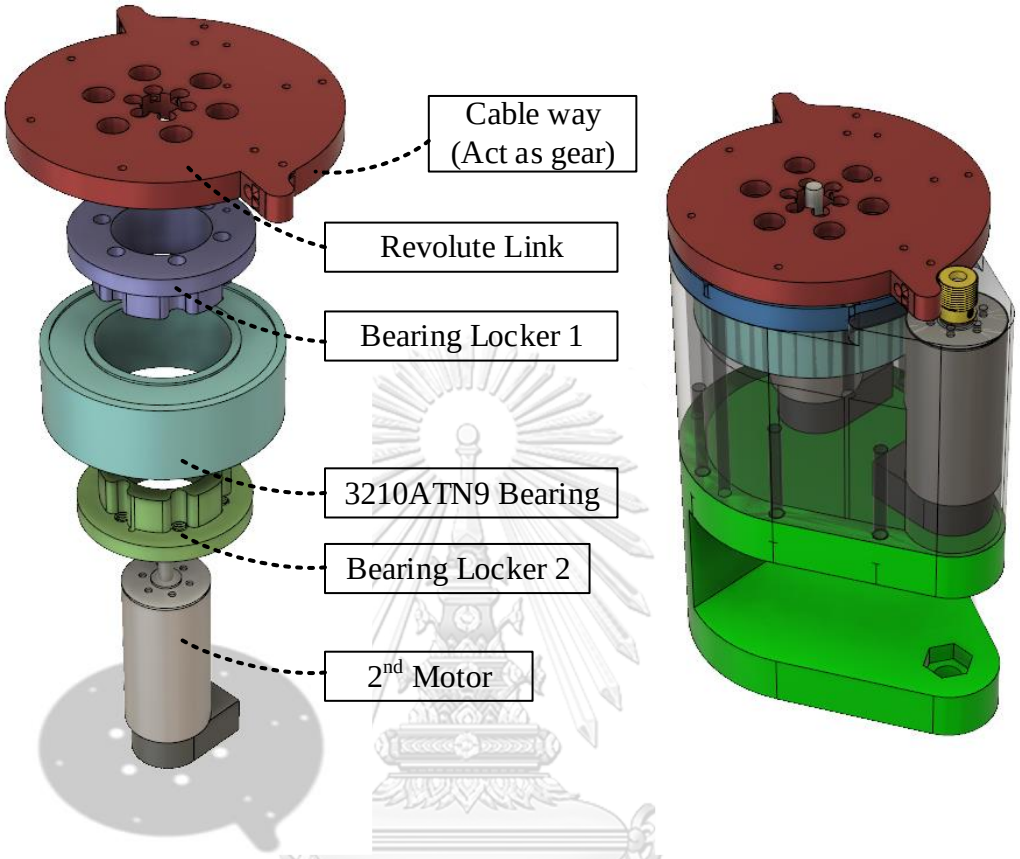

Figure 3.6 Revolute link parts before assembled (left), assembled (right).

Figure 3.7 Revolute joint cable transmission

3.1.4.4 Prismatic Joint Design

Differs from the first prototype, the prismatic joint of this design works by mounting linear rail on the revolute joint, and the prismatic cable drive is designed using the concept of timing belt instead of rack and pinion. The prismatic link, which is mounted on the Linear block, is designed to bind the cable and carry Force/Torque sensor.

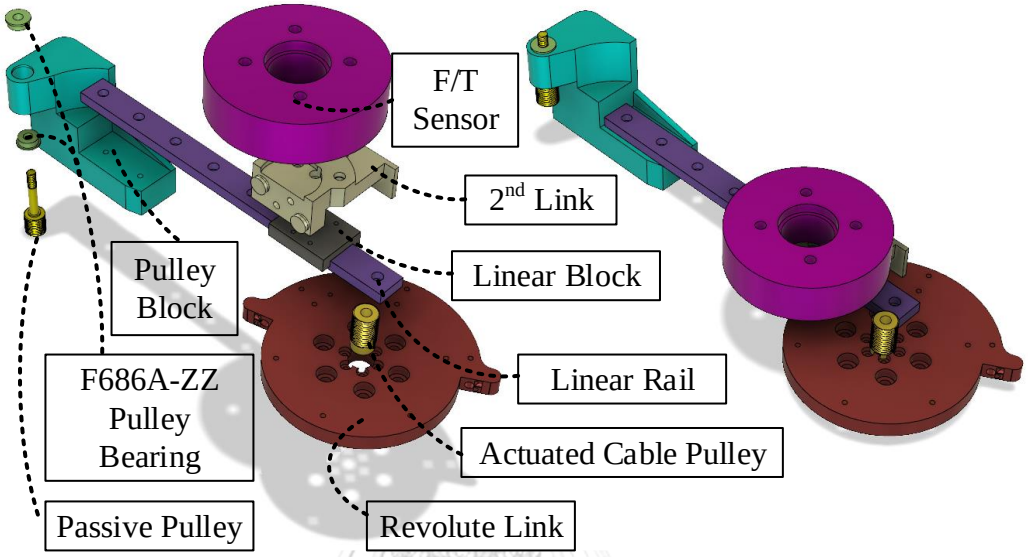

Figure 3.8 Prismatic link parts before assembled (left), assembled (right)

Figure 3.9 Pulley mover of prismatic joint

3.1.4.5 Passive Joint Design

The passive joint is a non-actuated low friction revolute joint located on the end effector used to avoid interference due to differences between human and robot kinematics.

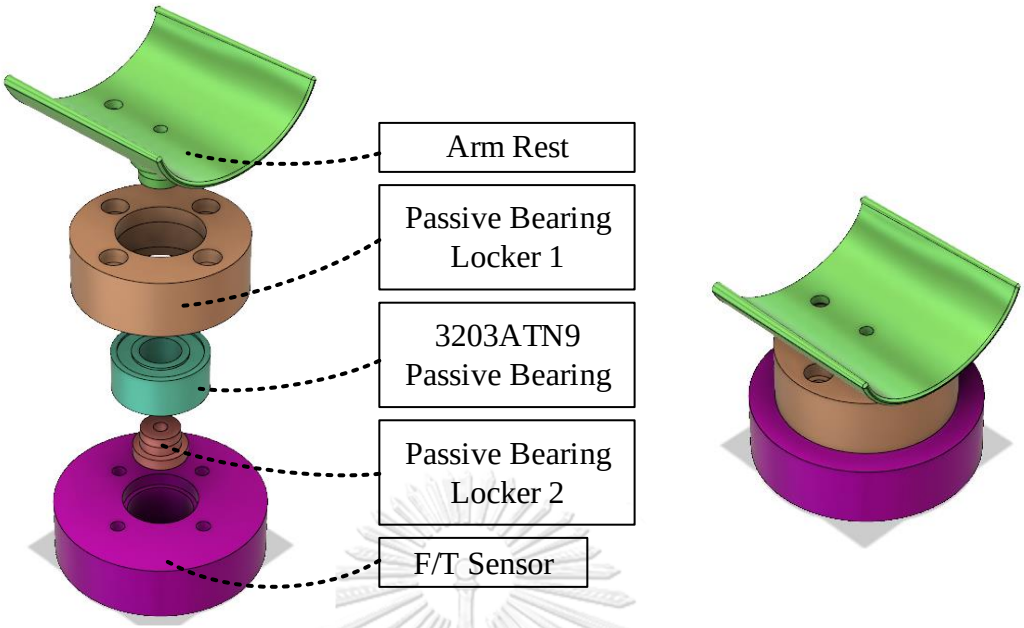

Figure 3.10 Passive joint parts before assembled (left), assembled (right)

3.1.4.6 Overall Specification

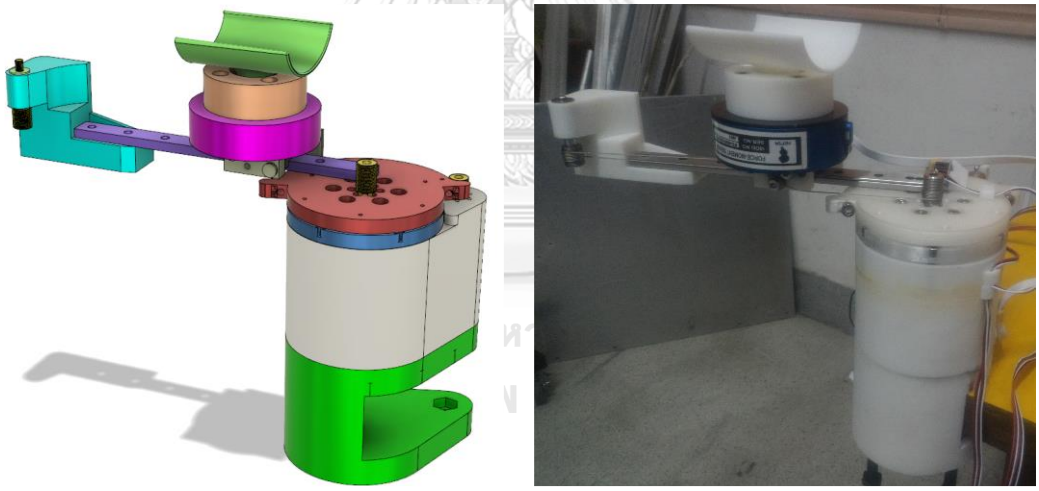

Figure 3.11 Second prototype design CAD (left), built model (right).

Table 3.3 Second prototype specification

Specification	Value
Revolute joint designed approximated reduction ratio	64/7 = 9.142857
Revolute joint measured reduction ratio	9.207467
Revolute joint position resolution (degree)	0.001954935
Revolute joint designed range (degree)	0 to 135
Prismatic joint designed approximated ratio (mm/rev)	43.982297
Prismatic joint measured ratio (mm/rev)	44.475535
Prismatic joint position resolution (mm)	0.002223776762335
Prismatic joint designed range (mm)	27.875 to 207.875

3.2 Controller System Design

The control system used in this research is Simulink Real-Time, implemented on an x86 PC with I/O cards.

3.2.1 Electronics Design

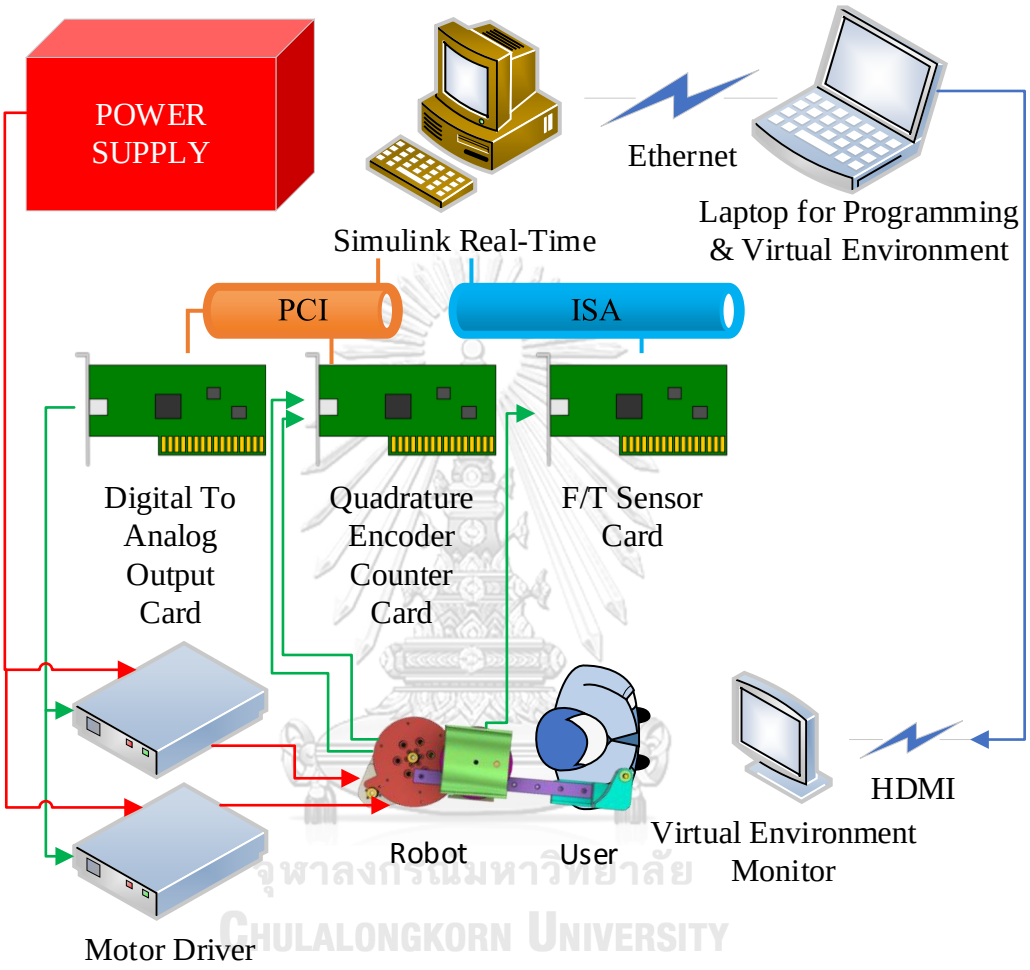

Figure 3.12 Electronics diagram

3.2.2 Mathematics of the Robot.

To derive mathematics of the robot, frames and space must be defined. Because this end-effector robot is not able to observe user pose precisely, all mathematics are derived with the assumption that the user is at pose for horizontal flexion/extension and the shoulder location is fixed.

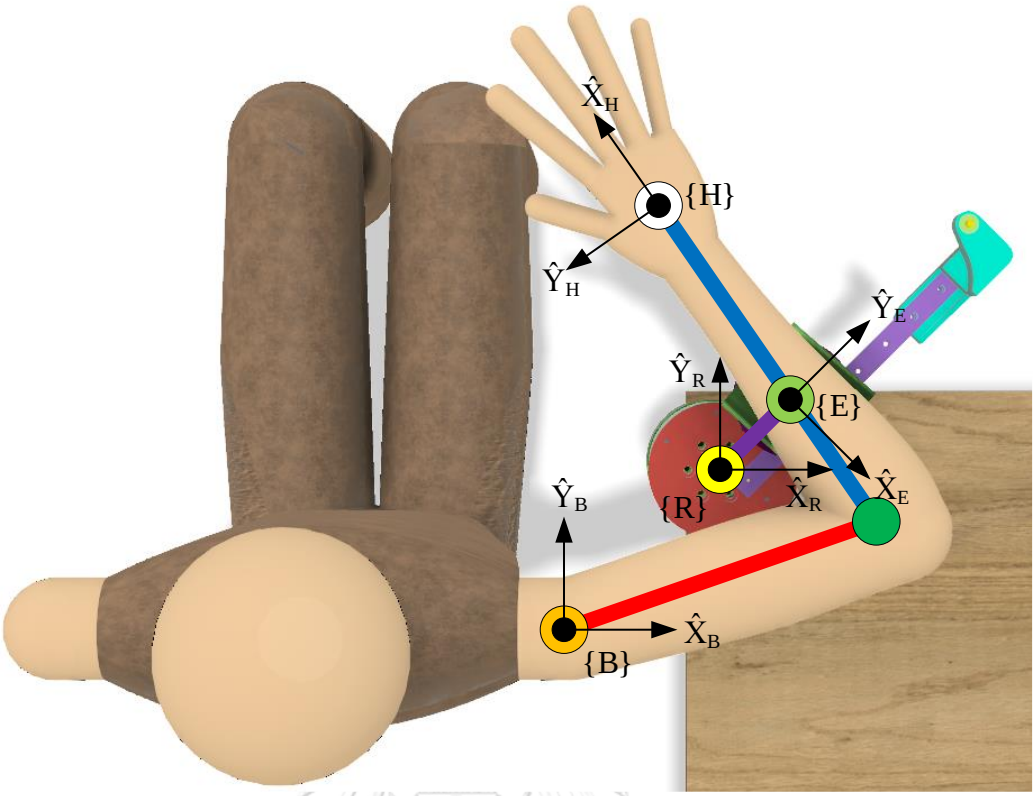

Figure 3.13 Defined frame of the robot

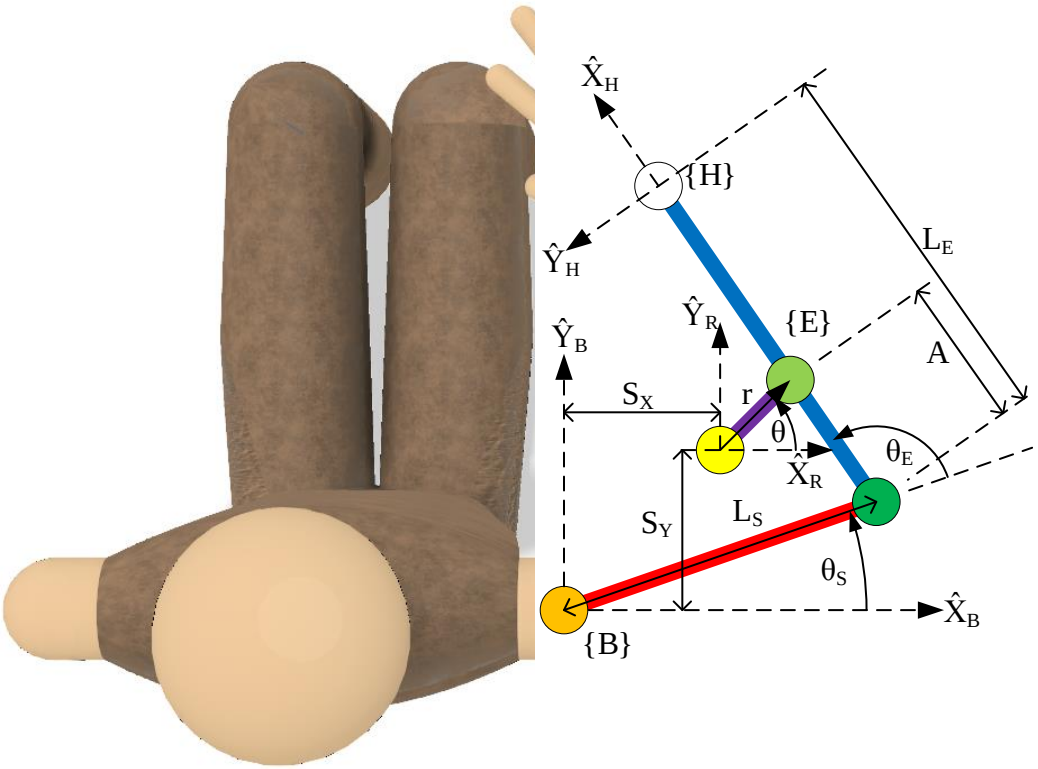

Figure 3.14 Defined variable and parameter of the robot

There are 3 frames attached to the robot as shown in Figure 3.13.

1. Base frame (B frame, a stationary frame), located at the shoulder.
2. Robot frame (R frame, a stationary frame), located at the robot revolute joint.
3. End-effector frame (E frame, a moving frame), located at the end-effector.

Variables and parameters used in mathematics are shown in Figure 3.14.

Table 3.4 Defined variables and parameters of the robot.

Denoted	Definition	Value
L_S	Upper arm length (Shoulder to elbow)	250 mm
L_E	Forearm length (Elbow to hand center)	300 mm
A	Elbow to end-effector length	120 mm
S_X	Robot displacement from the shoulder, in the X direction	110 mm
S_Y	Robot displacement from the shoulder, in the Y direction	110 mm
R_R	The reduction ratio of the rotation joint.	9.21
R_P	Nominal cable pinion radius of prismatic joint	7.08 mm
θ	The angular position of robot revolute joint.	Variable
r	Linear position of robot prismatic joint (From robot center to end-effector)	Variable
Θ	Joints position vector (θ and r)	Variable
θ_S	Shoulder horizontal flexion angle	Variable
θ_E	Elbow flexion angle	Variable
${}^R E_X$	The position of End-effector in the X direction of R frame	Variable
${}^R E_Y$	The position of End-effector in the Y direction of R frame	Variable
${}^B E_X$	The position of End-effector in the X direction of B frame	Variable
${}^B E_Y$	The position of End-effector in Y direction of B frame	Variable
${}^B H_X$	The position of Hand in the X direction of B frame	Variable
${}^B H_Y$	The position of Hand in the Y direction of B frame	Variable
F_X	Force applied to the arm in the X direction of B frame	Variable
F_Y	Force applied to the arm in the Y direction of B frame	Variable
${}^E F_X$	Force applied to the arm in the X direction of E frame	Variable
${}^E F_Y$	Force applied to the arm in the X direction of E frame	Variable
τ_1	Motor 1 (Revolute) torque	Variable
τ_2	Motor 2 (Prismatic) torque	Variable
τ_R	Revolute joint torque (CCW)	Variable
F_P	Prismatic joint force, Y direction of E frame	Variable
τ_S	Shoulder torque in Horizontal Flexion motion.	Variable
τ_E	Elbow torque in Elbow Flexion motion	Variable

The upper arm and forearm length used are measured from the author's arm.

Because incremental encoders mounted at the rear of the motors are used as position sensors, the measured position is in joint space frame $[\theta, r]$. All other variables can be derived using forward kinematic.

The equations of forward kinematic are

$$ {}^{R}E_X = r\cos\theta \tag{3.1} $$

$$ {}^{R}E_Y = r\sin\theta \tag{3.2} $$

$$ {}^{B}E_X = {}^{R}E_X + S_X \tag{3.3} $$

$$ {}^{B}E_Y = {}^{R}E_Y + S_Y \tag{3.4} $$

$$ \theta_E = \operatorname{acos}\left(\frac{{}^{B}E_X^2 + {}^{B}E_Y^2 - L_S^2 - A^2}{2L_S A}\right) \tag{3.5} $$

$$ \theta_S = \operatorname{atan2}\left({}^{B}E_Y, {}^{B}E_X\right) - \operatorname{atan2}(A\sin\theta_E, L_S + A\cos\theta_E) \tag{3.6} $$

$$ {}^{B}H_X = L_S\cos\theta_S + L_E\cos(\theta_S + \theta_E) \tag{3.7} $$

$$ {}^{B}H_Y = L_S\sin\theta_S + L_E\sin(\theta_S + \theta_E) \tag{3.8} $$

The equations (3.1) - (3.8) defined forward kinematic of the whole system (from joint positions toward hand positions). The inverse kinematic, from hand positions to joint positions, can be derived by following equations.

$$ \theta_E = \operatorname{acos}\left(\frac{{}^{B}H_X^2 + {}^{B}H_Y^2 - L_S^2 - L_E^2}{2L_S L_E}\right) \tag{3.9} $$

$$ \theta_S = \operatorname{atan2}\left({}^{B}H_Y, {}^{B}H_X\right) - \operatorname{atan2}(L_E\sin\theta_E, L_1 + L_E\cos\theta_E) \tag{3.10} $$

$$ {}^{B}E_X = L_S\cos\theta_1 + A\cos(\theta_S + \theta_E) \tag{3.11} $$

$$ {}^{B}E_Y = L_S\sin\theta_S + A\sin(\theta_S + \theta_E) \tag{3.12} $$

$$ {}^{R}E_X = {}^{B}E_X - S_X \tag{3.13} $$

$$ {}^{R}E_Y = {}^{B}E_Y - S_Y \tag{3.14} $$

$$ r = \sqrt{{}^{R}E_X^2 + {}^{R}E_Y^2} \tag{3.15} $$

$$ \theta = \operatorname{atan2}\left({}^{R}E_Y, {}^{R}E_X\right) \tag{3.16} $$

For force and torque calculation, since the nature of rehabilitation is very slow, force and torque from inertia which includes Coriolis and Centripetal are neglected and only calculate with massless assumption. If the user wishes to move faster, the user will experience resisting inertia and friction from both the robot and his/her arm.

Due to Revolute-Prismatic configuration, with the robot mass neglected, force exerts on the arm at the end-effector in E frame are decoupled from each other as shown in the following equations.

$$ {}^{E}F_X = -\frac{\tau_R}{r} = -\frac{R_R \tau_1}{r} \tag{3.17} $$

$$ {}^{E}F_Y = F_P = \frac{\tau_2}{R_P} \tag{3.18} $$

$$ F = \begin{bmatrix} F_X \\ F_Y \end{bmatrix} = {}^{B}_{E}R \, {}^{E}F = \begin{bmatrix} \cos\theta & -\sin\theta \\ \sin\theta & \cos\theta \end{bmatrix} \begin{bmatrix} {}^{E}F_X \\ {}^{E}F_Y \end{bmatrix} \tag{3.19} $$

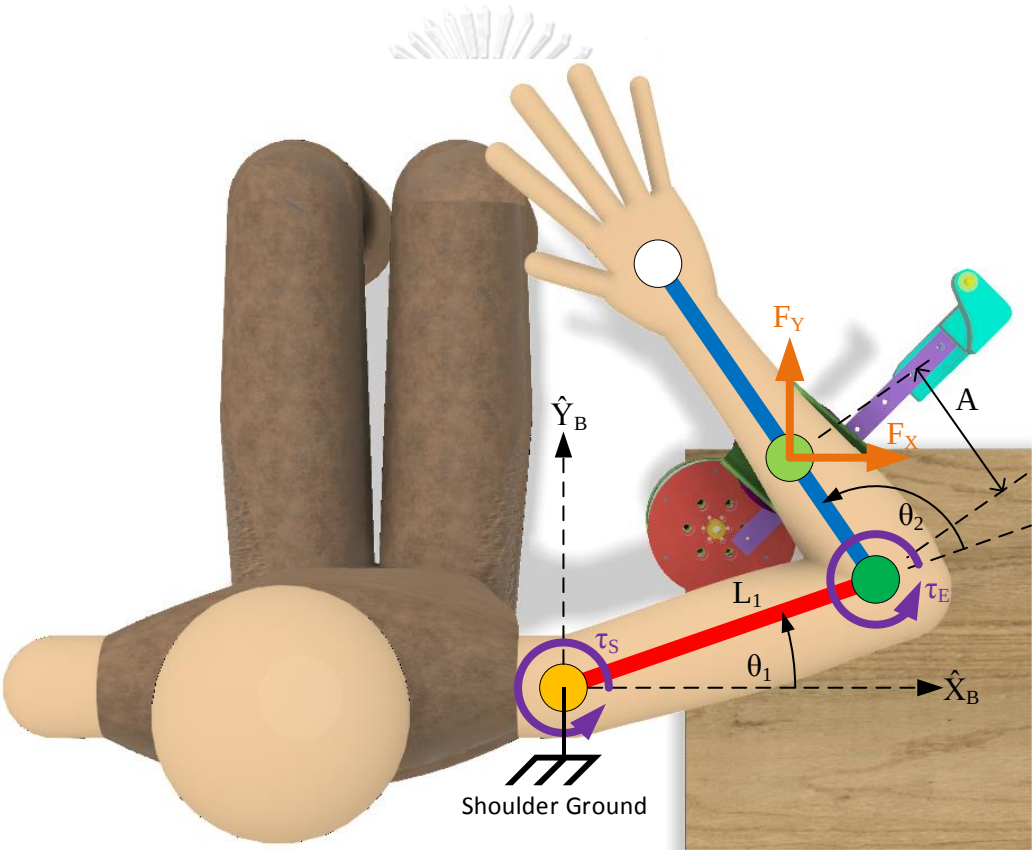

Figure 3.15 Free body diagram of the arm.

From the free body diagram, force the robot applied to the arm is a function of shoulder and elbow torques exerted by a human.

$$ \tau_E = A(F_X \sin(\theta_S + \theta_E) - F_Y \cos(\theta_S + \theta_E)) \tag{3.20} $$

$$ \tau_S = \tau_E + L_S(F_X \sin(\theta_S) - F_Y \cos(\theta_S)) \tag{3.21} $$

And the inverse function is

$$F_{T1} = \frac{(\tau_S - \tau_E)}{L_S} \tag{3.22}$$

$$F_{T2} = \frac{F_{T1}\cos\theta_E - \tau_E}{\sin\theta_E} \tag{3.23}$$

$$F_X = F_{T1}\sin\theta_S - F_{T2}\cos\theta_S \tag{3.24}$$

$$F_Y = -F_{T1}\cos\theta_S - F_{T2}\sin\theta_S \tag{3.25}$$

3.2.3 Control Laws

3.2.3.1 Position Controller

The position controller is used mainly for passive rehabilitation. The position controller is designed as an independent joint control. The position controller uses reference hand position in the task space cartesian frame as a command and drive out motors torque. The encoders are used as feedback signals.

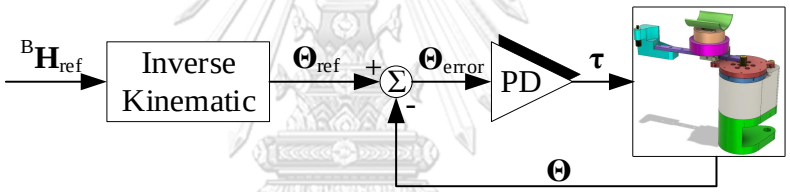

Figure 3.16 Position controller diagram.

The position controller converts the reference position from the task space cartesian frame into reference joint position. From the joint positions, closed-loop PD controllers are used. Because both motors are identical, PD gains are chosen the same for both motors. The PD gains are tuned at the 2nd motor to maximum stable stiffness, then transform into corresponding 1st motor gains such that the impedances at the motors are the same. The stiffness of gains is limited by noise from derivatives and sampling rates, which is 1kHz. From an experiment, the 2nd prototype robot is very fast and can vibrate up to 0.5kHz, due to low inductance and low inertia of coreless brushed DC motor.

3.2.3.2 Force Controller

Intent-based assistive active rehabilitation needs to sense user intent to move. The user intent can be measured by the Force/Torque sensor. The 1st prototype has been implemented with this type of rehabilitation [21]. The concept is to store force generated by user intent and use it to assist motion. The controller in [21] uses an integral controller, which will assist until stopping intent is observed. This controller is called a force amplifier because the side effect is minimizing interaction force between the robot and the user. Utilizing integral controller result in integral of force over time will be bounded. However, the energy provided by the robot is not constrained. This

mode assistance concept is to absorb force at low velocity (low power is absorbed) and releases assistance force at higher velocity (high power is released).

The intent based assistive implemented on the 2nd prototype will be based on force amplifier implemented before. The major change is to decrease assistance force if the user shows no intent. This change is done by using a time delay with a proportional controller instead of an integral controller. With this controller, the user must show small intention all the time while moving. The assistance concept will be almost the same as integral control, but the assistance force is asymptotically bounded.

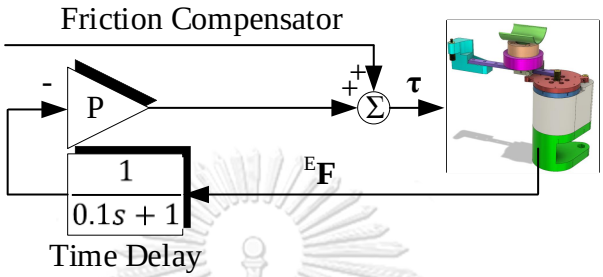

Figure 3.17 Force controller diagram

3.2.3.3 Friction Compensator

To increase the performance of the controllers, the robot friction needs to be compensated. Simplified friction dynamic is composed of Coulomb and Viscous friction, which are functions of velocity. Because velocity used to estimate is derived from encoders, which introduces noise, using this derived velocity to estimate friction will create very large noise. To solve this problem, a low pass filter is used for friction estimator. Deadband is used to filter out low velocity, and saturation is used to limit velocity to unit vectors. Since robot joints friction are decoupled to dedicate motors, friction compensation can be calculated separately for each motor and encoder.

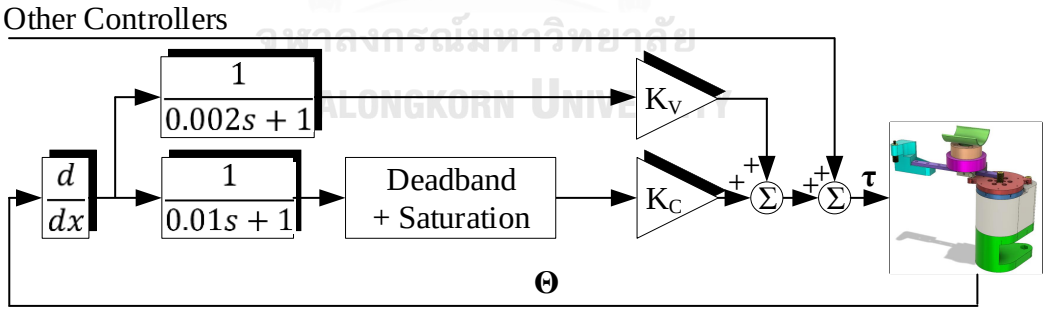

Figure 3.18 Friction compensator diagram

The K_V, viscous gain, and K_C, coulomb gain, are chosen at half the unstable gains. The more accurate these gains are, the higher the performance. But higher gains than actual gains will leads to instability.

3.2.4 Electromyography Measurement Unit Design

In this research, four muscles sEMG will be observed. Because the real voltage of sEMG is very low and need a high gain amplifier, the measurement unit must be totally isolated from every power source.

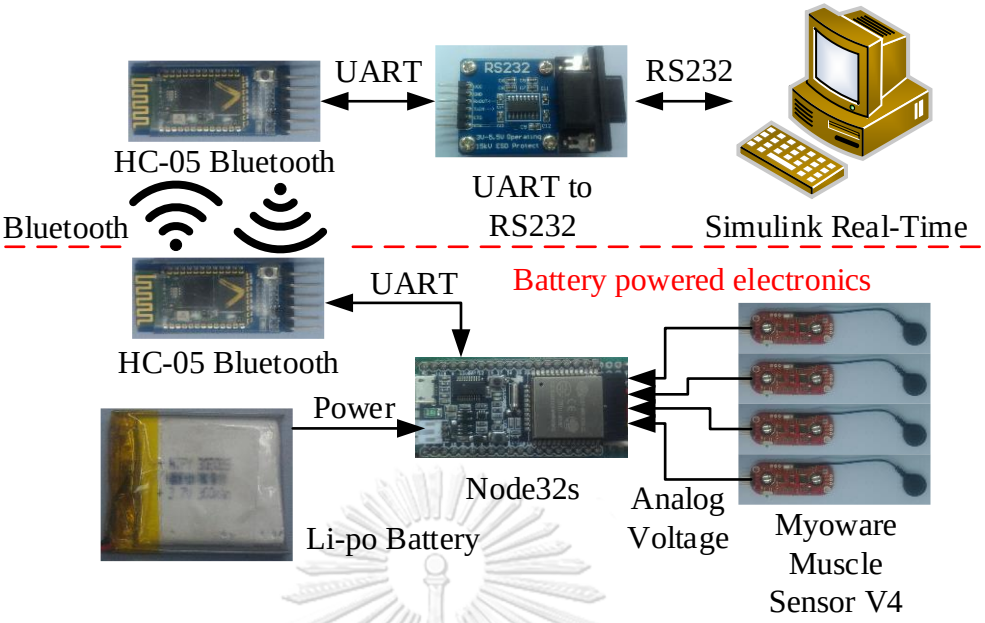

Figure 3.19 sEMG measurement unit diagram

The sEMG measurement unit utilizes Myoware Muscle Sensor v4 for amplifying sEMG signals from muscles. The unit read signal values and send to Simulink Real-Time system via Bluetooth.

Since there are more than one muscles responsible for each motion, each of the observed muscles are chosen only one muscle per motion.

The four observed muscles are

1. Pectoralis Major, primary muscle for shoulder horizontal flexion.
2. Deltoid Posterior, primary muscle for shoulder horizontal extension.
3. Biceps Brachii, primary muscle for elbow flexion.
4. Triceps Lateral, primary muscle for elbow extension.

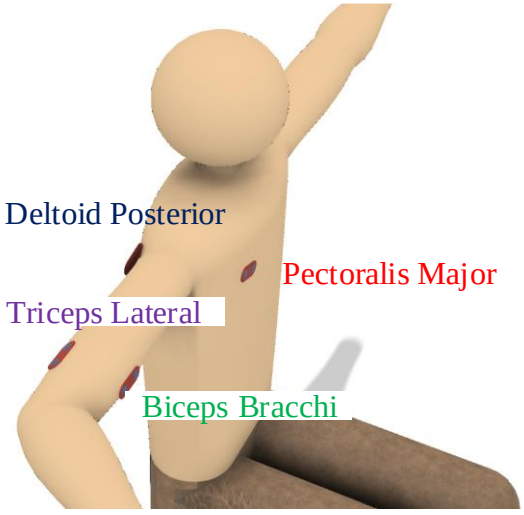

Figure 3.20 Installed position of sEMG sensors.

3.3 Virtual Environment Design

To operate the robot efficiently, a virtual environment is needed. From reviews in the second chapter, mostly rehabilitation task is reaching task. The virtual environment can be either an activity or game-based. However, a game based has advantages that difficulty can be adjusted.

A game based virtual environment is proposed as a simple pick and place game, aimed to train the user in reaching task. The game objective is simple, the user needs to select a ball in a game, and then reach out his/her hand to pick it. The user can pick up the ball by hovering his/her arm over the ball for 2 seconds. If the user's hand is correctly above the ball, the white circle will slowly turn red and switch to blue when 2 seconds is reached. The user will be able to tell that the ball is grabbed when in-game fingers are flexed. After grabbing a ball, the user needs to bring the ball to the blue circle, which is close to the user body. When the grabbed ball touches the blue circle, the hand will release, and the ball disappears, the user needs to reselect other balls.

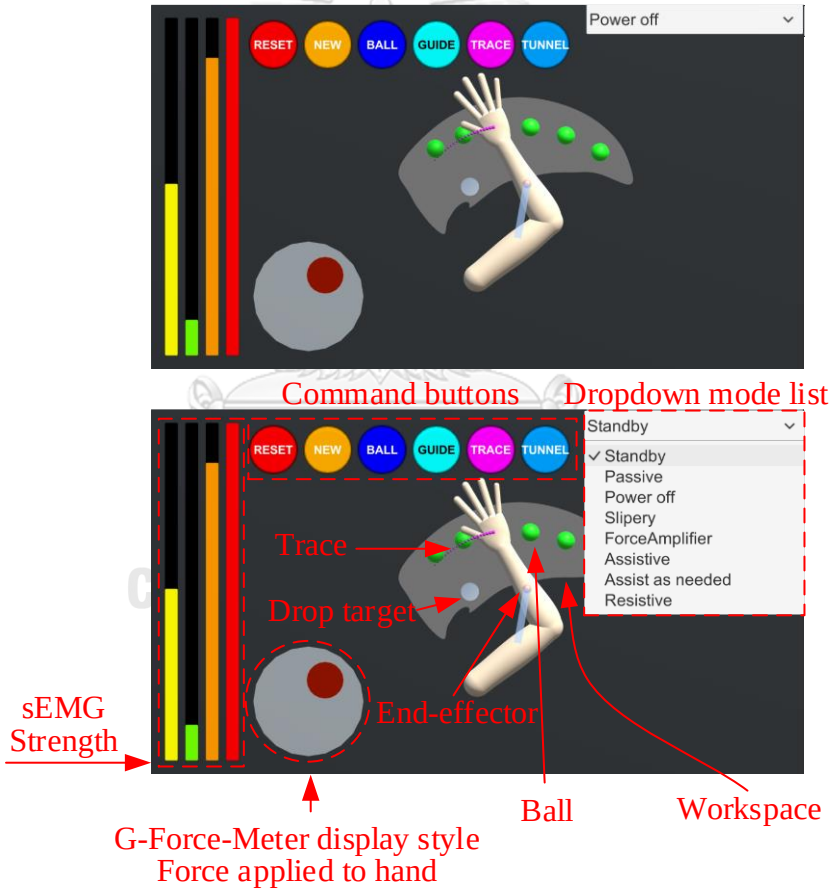

Figure 3.21 Proposed Virtual Environment for rehabilitation.

Not only giving tasks to the user, the virtual environment also has UI which can display and switch between operation modes.

There are 4 sEMG gauges displays on the left side of the game. The interaction forces the robot is pushing the user's arm is displayed at the bottom left, next to sEMG gauges. The interaction force is displayed similar way G-force sensor does. The

estimated arm pose is also displayed in the game, and the user can move it like his/her own arm. The robot pose is shown in the game as a transparent blue bar as robot link and a transparent pink ball as end-effector. The trace of hand center movement is also shown in the game as small pink balls, but the user can disable it. When a target ball (blue) is selected, the game shows a transparent cyan linear path between hand center and the ball, but the user can disable this option.

There are 6 buttons in the game which control both the game and the robot.

RESET: Restart the robotic system.

NEW: Start a new game, bring back all disappear balls.

BALL: Select a ball, click once and one of the balls will change its color into cyan. Clicking the button again will select another ball. When the button is not clicked for 3 seconds, the selected cyan ball will turn blue which means it is a selected target.

GUIDE: Turn on or turn off transparent cyan guide path to the selected ball.

TRACE: Turn on or off the trace of hand center.

TUNNEL: Turn on or off force-field tunnel, as in [6], toward the target. Not implemented in this research.

3.4 Rehabilitation Modes Design

There are 4 rehabilitation modes proposed at the moment, which are composed of controllers proposed in the previous section. The rehabilitation modes can be selected from the drop-down list at the top right corner of the VE.

1. Passive: This is a passive rehabilitation. When the target ball is selected, the robot will generate a straight reference hand trajectory from the current position to the ball position with 1st order interpolation (constant velocity profile). Then the robot moves the user hand along the trajectory. After the ball is grabbed, the robot will bring the user hand toward blue circle target and stop until the next ball is selected.
2. Power off: This is an active non-assist rehabilitation. The robot motors will not be driven, and the robot only provides bearing gravity support while the user moves his/her limb at will.
3. Slippery: This is an active non-assist rehabilitation. Different from the previous mode is that the robot provides friction compensation so that the user will experience less resist force.
4. Force Amplifier: This is an intent-based active assist rehabilitation. The robot will apply assistance force when the user show moves intent.

Only 4 rehabilitation modes are implemented in this research, but the VE is built such that the other modes can be implemented in the future. The other modes are

1. Assistive: This is a task-based active assist rehabilitation. The robot will apply constant assist force in the target direction.
2. Assist as needed: This is a task-based active assist rehabilitation concept which will let the user do the task and assist only when there is a need.

3. Resistive: This is a task-based active assist (resist) rehabilitation. The robot will apply constant resist force in the target direction.

CHAPTER 4
EVALUATION

The previous chapters describe the design of the rehabilitation robot system, controllers, and rehabilitation modes. This chapter will provide the results of the evaluation with 2 volunteered healthy subjects with all 4 proposed rehabilitation modes, 3 sets per subject. The evaluations were done by the subject do the task with all the 4 modes before redoing a new set. The real-time pose, interaction force (the force the robot applies to the arm at the end-effector, from F/T sensor), sEMG signals and other variables will be recorded and used to evaluate the system.

4.1 Evaluation Setup

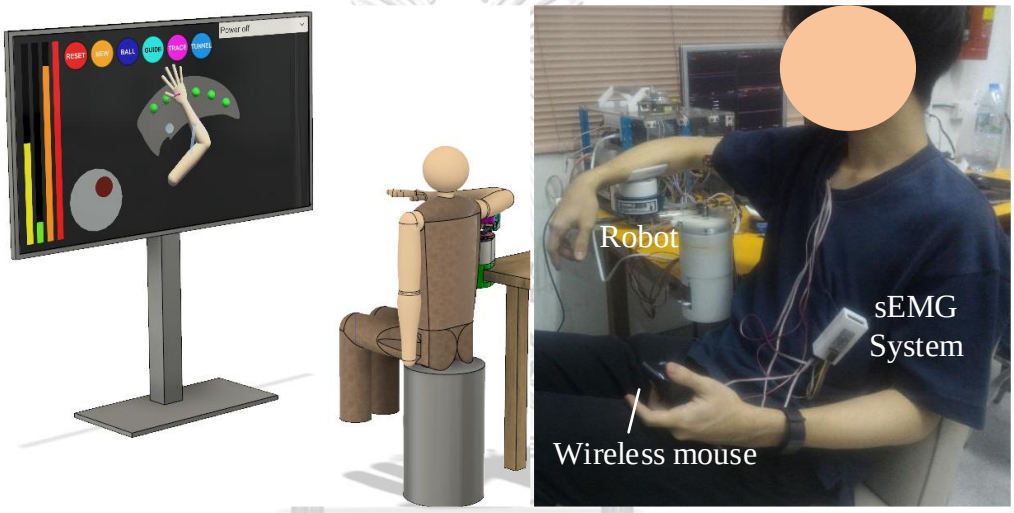

Figure 4.1 Evaluation Setup

The evaluation is done by having the robot install on the table side and have the subjects sit next to it. The sEMG measurement unit is installed to the subjects, measuring signals of Pectoralis Major, Deltoid Posterior, Biceps Brachii and Triceps Lateral. The VE monitor is set in front of the subjects with comfort distance. The operator then setup the VE and choose rehabilitation modes. During rehabilitation, the subjects choose the target ball by a wireless controller in his/her health hand. The task is to reach the target ball and bring the ball back, a total of 6 balls. Each subject playing the game for 3 sets, each set consists of 4 modes concluding a total 12 runs for each subject.

The position of the balls can be set. For this demonstration, the balls are distributed in a circular arc around the shoulder to cover most reachable space of the hand as in Figure 4.2.

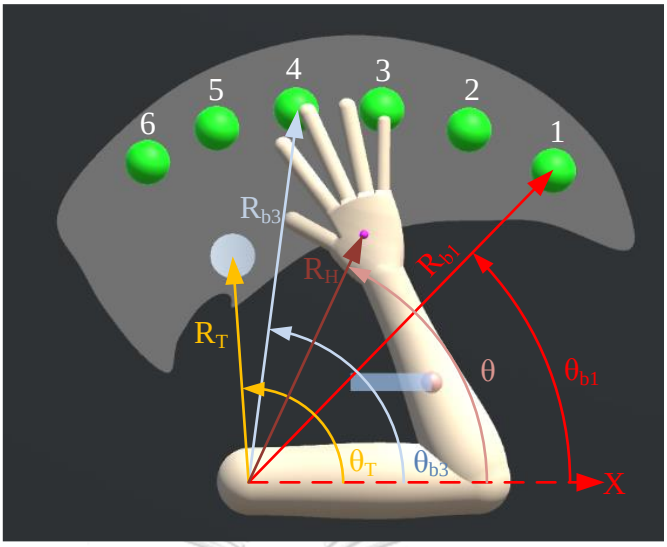

Figure 4.2 Balls and drop target placement

Table 4.1 Balls and drop target parameter

Target	Angle θ (degree)	Radius R (mm)
Ball 1 (b1)	45.837	480
Ball 2 (b2)	58.251	458
Ball 3 (b3)	70.665	437
Ball 4 (b4)	83.079	415
Ball 5 (b5)	95.493	393
Ball 6 (b6)	107.91	372
Drop Target (T)	94.570	251

4.2 Evaluated Criterions.

To prove the reliability of the proposed rehabilitation system, the results from both subjects should not differ much. They should appear similarly and leads to the same conclusion.

Table 4.2 Criterions for evaluation.

Mode	Criterion	Evaluate on
Passive	Small position error.	Robot actuator strength. Position controller.
Power off	Small interaction force.	Robot's backdrivability.
Slippery	Interaction force is smaller than Power off.	Friction compensator.
Force Amplifier	The robot assists the subjects.	Force amplifier controller.

4.3 Evaluation Result

Only the data from the first set of the subject A will be shown in graphical figures. In the first set, the subject A choose the balls in the order <1, 3, 5, 6, 2, 4> in every modes.

4.3.1 Result of the Passive Mode Evaluations

The passive mode has been evaluated with 30 mm/s hand velocity. The robot is able to drag the subject's arm along a straight-line trajectory as in Figure 4.3. In the first set of the subject A, the subject chooses the 1st ball as the first target. This makes the reference trajectory line cut through the workspace border, which is a non-convex workspace. When this happens, the controller drags the subject's arm along the workspace boundary instead. The robot's joints did not contact mechanical stoppers since there are soft joint limit controllers implemented in the system. However, the position controller does not know of the soft joint limit controller, which is the reason that the position error in Figure 4.4 becomes large. In the other cases, the position controller is able to drag the arm along reference trajectory with position error at the end-effector less than 6 mm. The position error in X_E (axial) is larger than the position error in Y_E (radial). The robot system can drive each motor up to 1.5 A, but the robot uses less than 0.4 A during the evaluation as in Figure 4.5.

During passive mode, the subjects were asked to rest the arm. However, there are changes in sEMG signals as in Figure 4.6. The sEMG sensor observing Pectoralis major picks up large rhythmic noise with frequency resemble the heartbeat as shown in Figure 4.7. However, this rhythmic noise has a constant amplitude. The observed sEMG during passive mode seems to pick up signals in conditions as in Table 4.3.

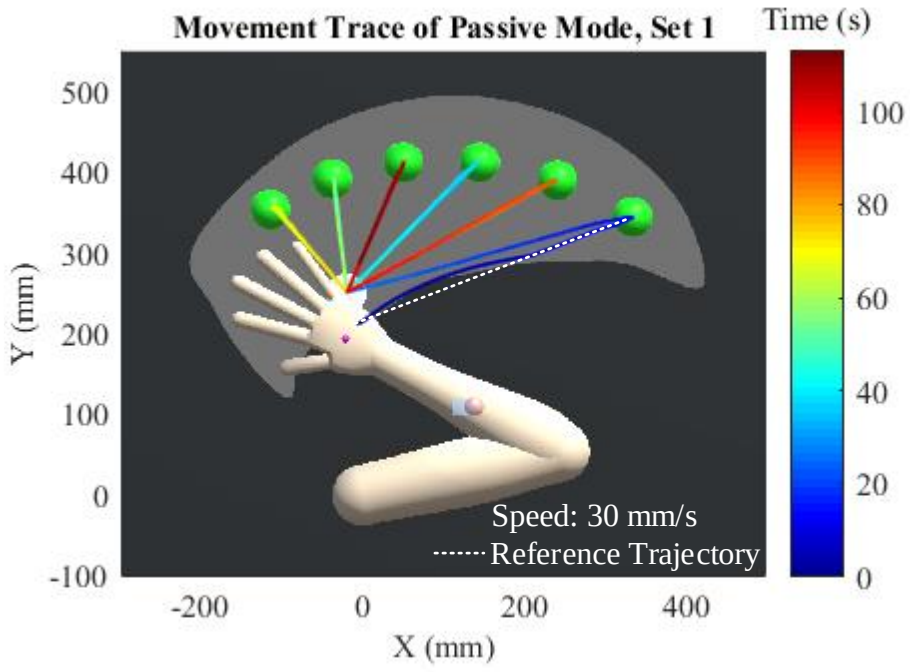

Figure 4.3 Movement trace during task performance in passive mode.

End-effector position error during passive mode.
Subject A, Set 1.

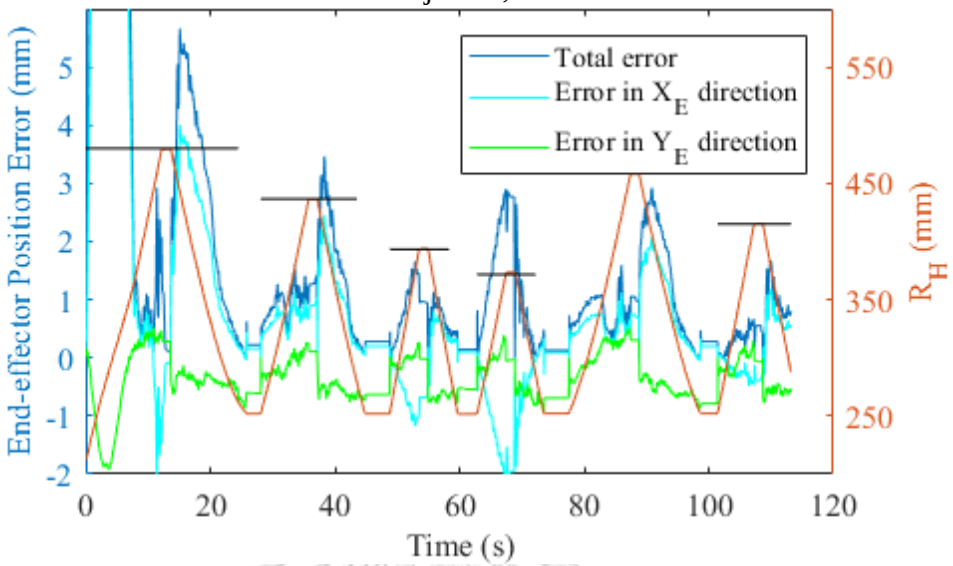

Figure 4.4 Position errors during passive mode evaluation.

Motor current during passive mode.
Subject A, Set 1.

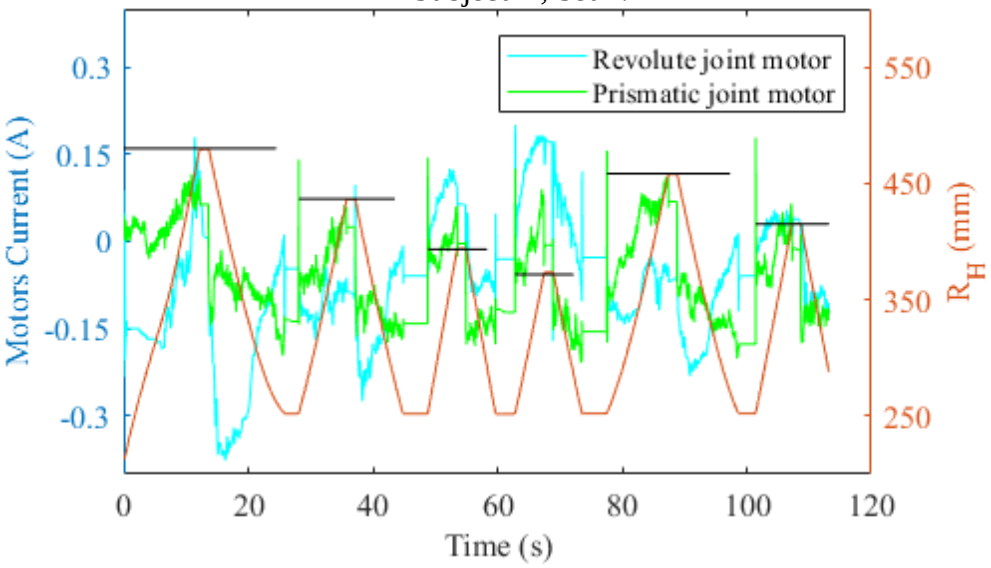

Figure 4.5 Motors current during passive mode evaluation.

Data from passive mode evaluation.
Subject A, Set 1.

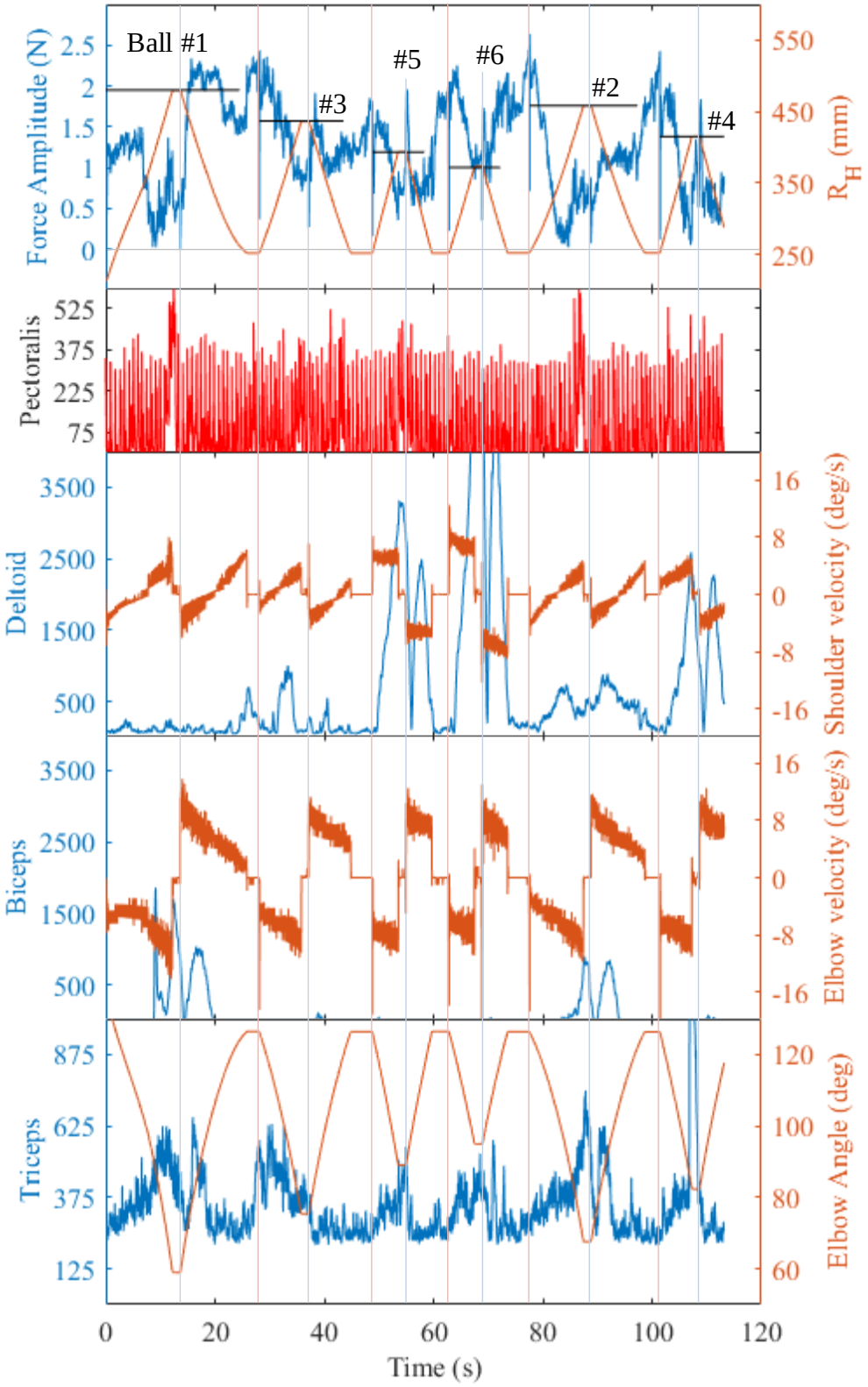

Figure 4.6 Data obtained during passive mode, subject A, set 1.

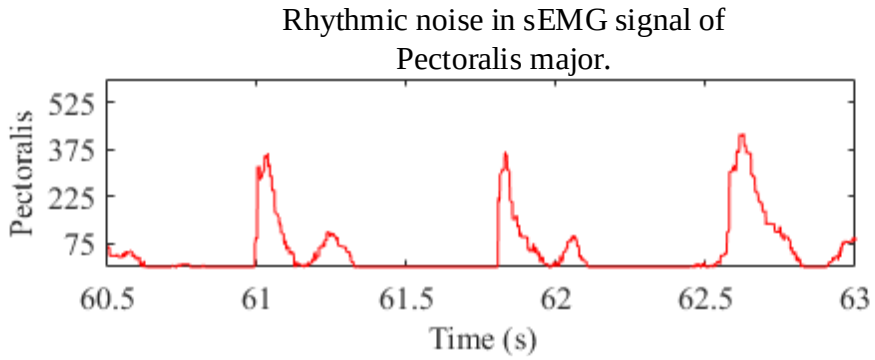

Figure 4.7 Rhythmic noise in sEMG signal.

Table 4.3 Observed sEMG characteristics in passive mode.

	High sEMG conditions in passive mode.					
Muscle	Shoulder joint			Elbow joint		
	Angle	Velocity	Acceleration	Angle	Velocity	Acceleration
Pectoralis major	Low	-	Large negative	-	-	-
Deltoid posterior	High	-	Large negative	-	-	-
Biceps brachii	-	-	-	Low	-	Large positive
Triceps lateral	-	-	-	Low	Negative	-

From Figure 4.6, the robot still applies force on the arm even there is no motion as the subject is asked to rest the arm. It seems that there is a static force relates to a pose. This static force is an internal force generated from the human arm and seems to be varying largely with hand position. The interaction force is converted into static shoulder and elbow torques using equations (3.20)-(3.21). Figure 4.8 and Figure 4.9 shows the calculated shoulder and elbow torques. It seems that when the subject has no movement intent, there still be joint passive torques relate to respective joints angle. The relation seems to be negatively proportional which makes the joint angle asymptotically stable around normal pose.

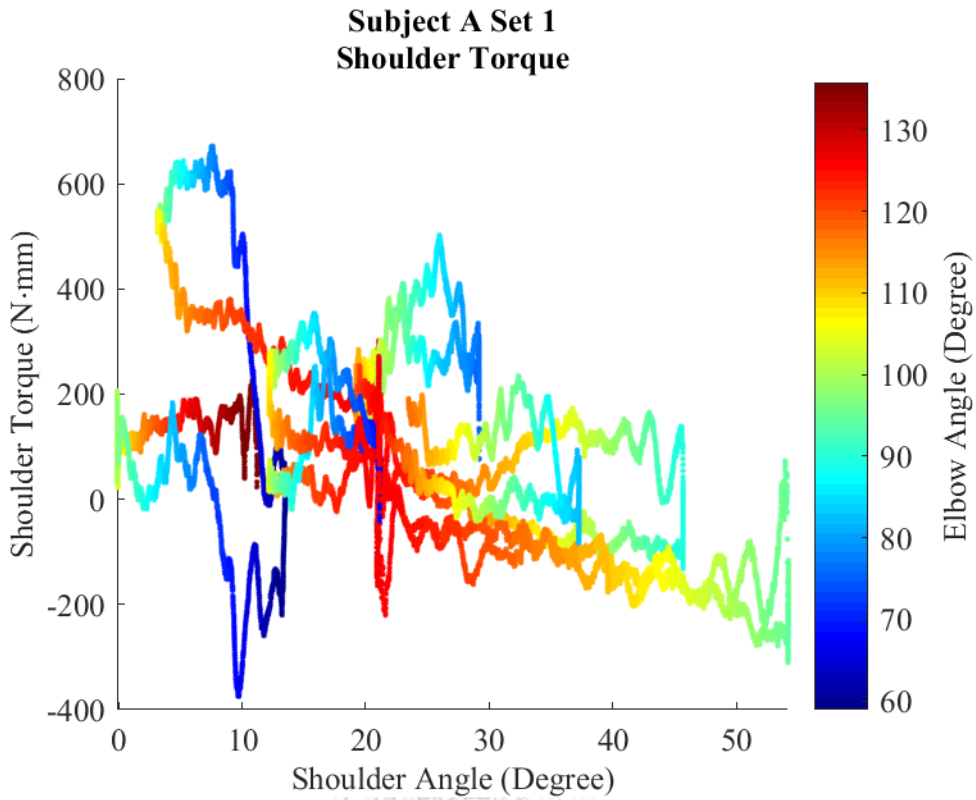

Figure 4.8 Shoulder torque during the passive mode.

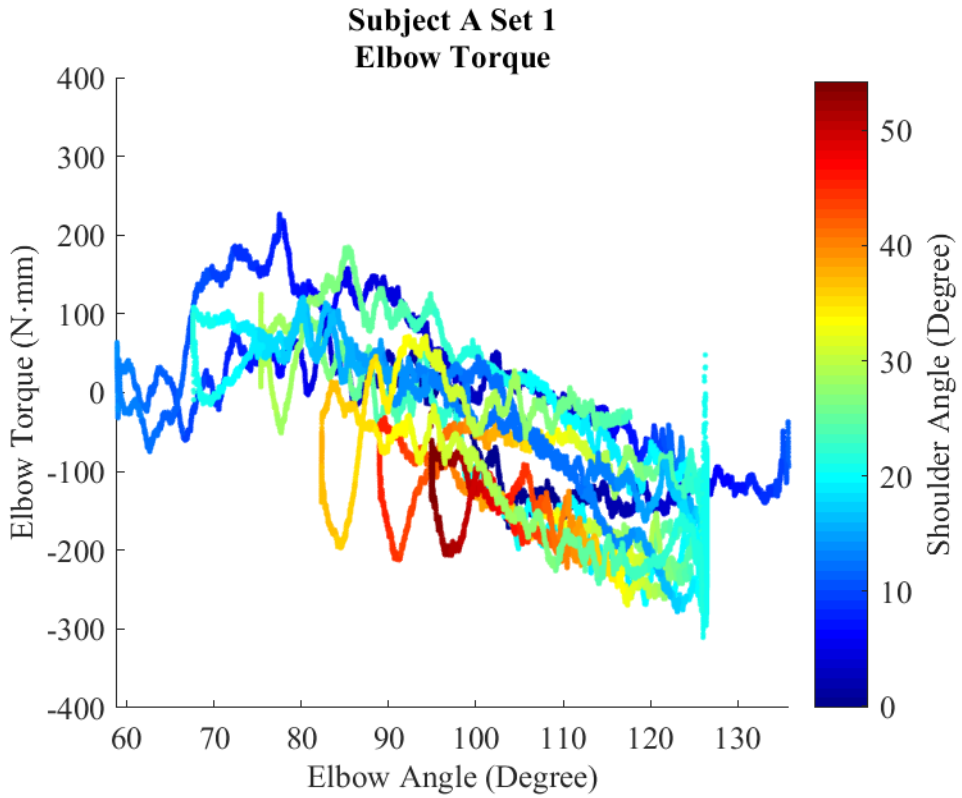

Figure 4.9 Elbow torque during the passive mode.

4.3.2 Results of the Power Off Mode Evaluations.

During power off mode evaluation, the robot only provides gravity compensation while the subjects do the tasks. In the first set of the subject A, the subjects experience interaction force in horizontal plane 1.17 N RMS (Table 4.4). The subjects are able to do the tasks with maximum hand velocity up to 200 mm/s as shown in Figure 4.10. The energy loss in dragging the robot is 1733 mJ (Table 4.6). The robot's assisted energy is work done to the subject arm at the end-effector, calculated from the interaction force and the motion of the end-effector. The negative assisted power means the robot is absorbing energy from the subject's arm. The robot-assisted power is mostly negative. The robot-assisted power is only positive when there is a braking action (sees Figure 4.11). The positive robot-assisted power does not generally means the robot is assisting the subject. The positive assisted power when braking means the robot is resisting braking action. It seems to be an effect from the robot inertia.

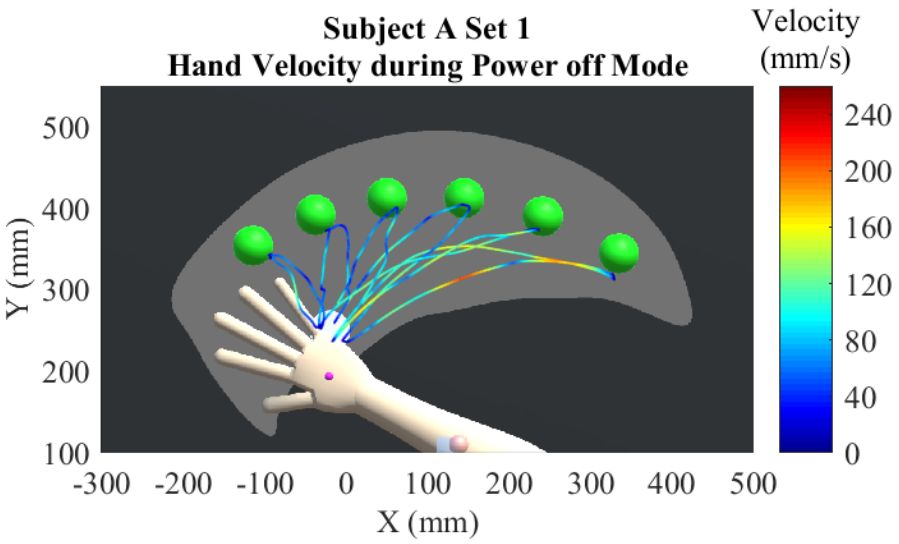

Figure 4.10 Hand velocity during power off mode evaluation.

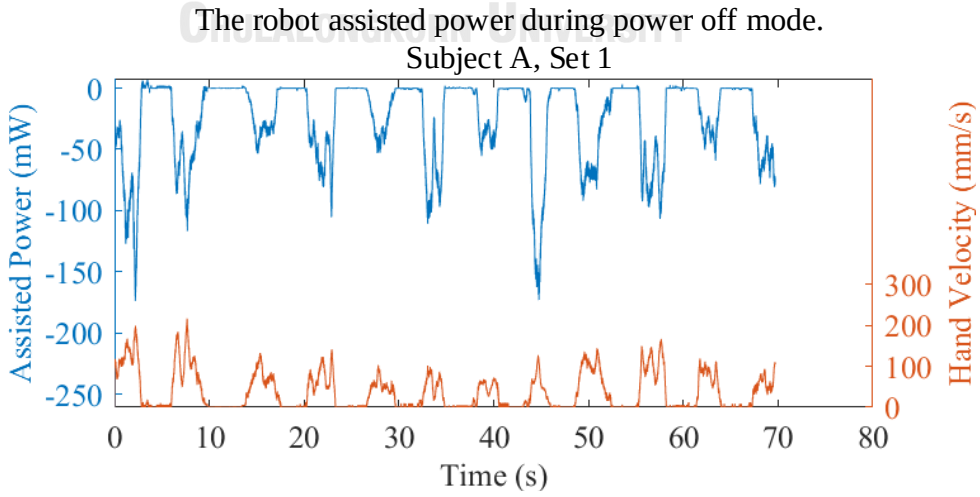

Figure 4.11 Robot-assisted power during power off mode evaluation.

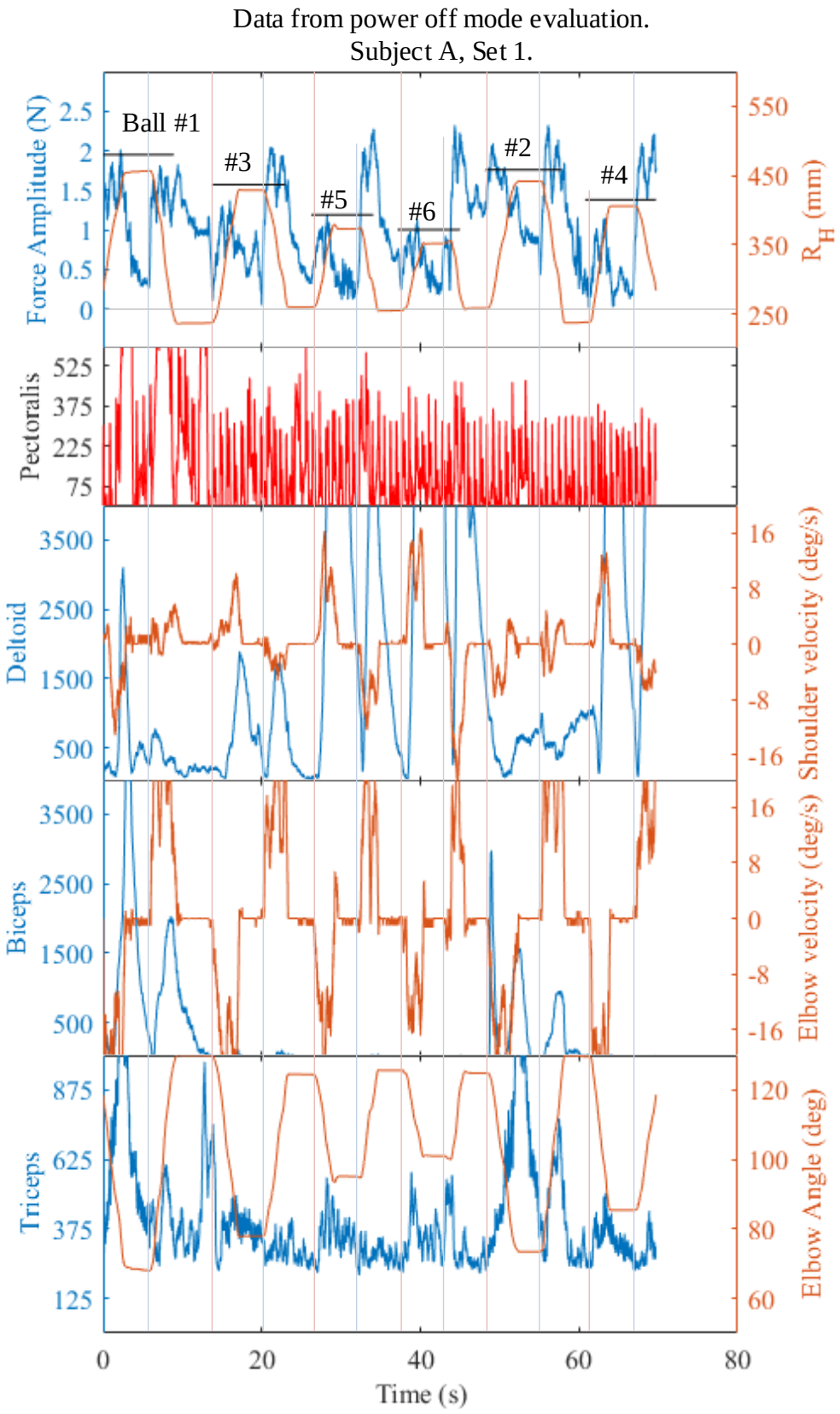

Figure 4.12 Data obtained during power off mode, subject A, set 1.

Table 4.4 Interaction force and time comparison.

Set	Set 1, Subject A		Set 2, Subject A		Set 3, Subject A	
	Force RMS (N)	Time (s)	Force RMS (N)	Time (s)	Force RMS (N)	Time (s)
Passive	1.39	113.19	1.47	119.19	1.03	109.34
Power off	1.17	69.70	1.13	79.66	1.23	77.66
Slippery	0.88	58.74	0.86	70.62	0.86	71.35
Force amplifier	0.22	61.24	0.26	65.66	0.26	70.01

Table 4.5 Total moving time during evaluation.

Total moving time (seconds), (Hand velocity > 15 mm/s)						
Mode	Subject A			Subject B		
	Set 1	Set 2	Set 3	Set 1	Set 2	Set 3
Passive	88.65	88.67	89.06	88.51	88.53	88.55
Power off	33.92	40.11	42.37	42.22	38.26	39.76
Slippery	29.74	33.77	36.14	36.71	35.09	27.82
Force amplifier	29.11	35.56	38.03	35.38	32.53	28.53

Table 4.6 Robot-assisted energy during active modes evaluations.

Robot-assisted energy (mJ)						
Mode	Subject A			Subject B		
	Set 1	Set 2	Set 3	Set 1	Set 2	Set 3
Power off	-1733	-1503	-1670	-1856	-1840	-1819
Slippery	-1131	-1177	-1197	-1398	-1429	-1253
Force amplifier	-243	-278	-302	-329	-323	-354

During the power off mode evaluation, the sEMG signals of 4 muscles are also observed as shown in Figure 4.12. However, the sEMG signal conditions are different than those in the passive mode. The sEMG signals of 4 muscles seem to have characteristics as shown in Table 4.7.

Table 4.7 Observed sEMG characteristics in power off mode.

	High sEMG conditions in passive mode.					
Muscle	Shoulder joint			Elbow joint		
	Angle	Velocity	Acceleration	Angle	Velocity	Acceleration
Pectoralis major	Low	-	Positive	-	-	-
Deltoid posterior	High	-	Negative	-	-	-
Biceps brachii	-	-	-	Low	-	Positive
Triceps lateral	-	-	-	Low	-	Negative

4.3.3 Results of the Slippery Mode Evaluation.

During the slippery mode evaluation of the subject A's 1st set, the subject did the task with hand movement velocity up to 240 mm/s (sees Figure 4.13). The total time and moving time is less than the power off mode (sees Table 4.4 and Table 4.5). The energy loss during the task is 1131 mJ (Table 4.6), which is less than the power off mode. The robot-assisted power is only positive when the subject does braking. This positive assisted power is larger than the power off mode.

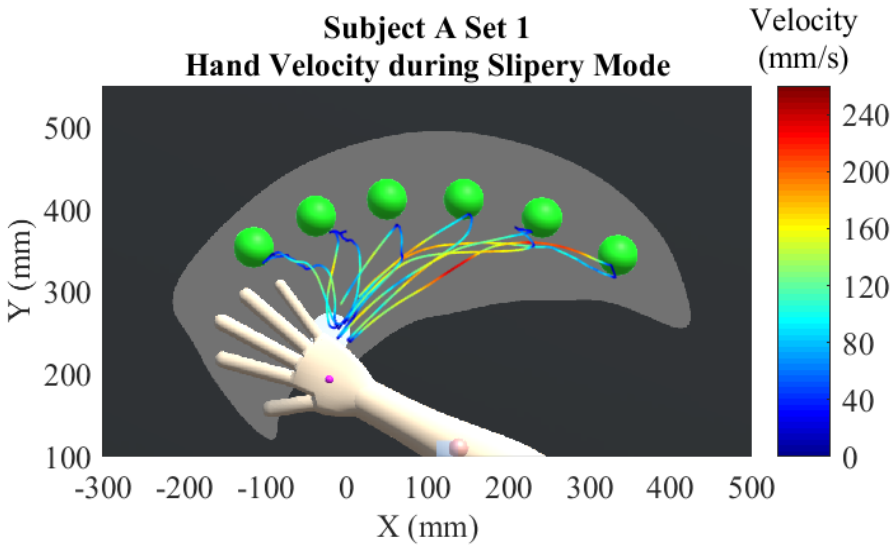

Figure 4.13 Hand velocity during slippery mode evaluation.

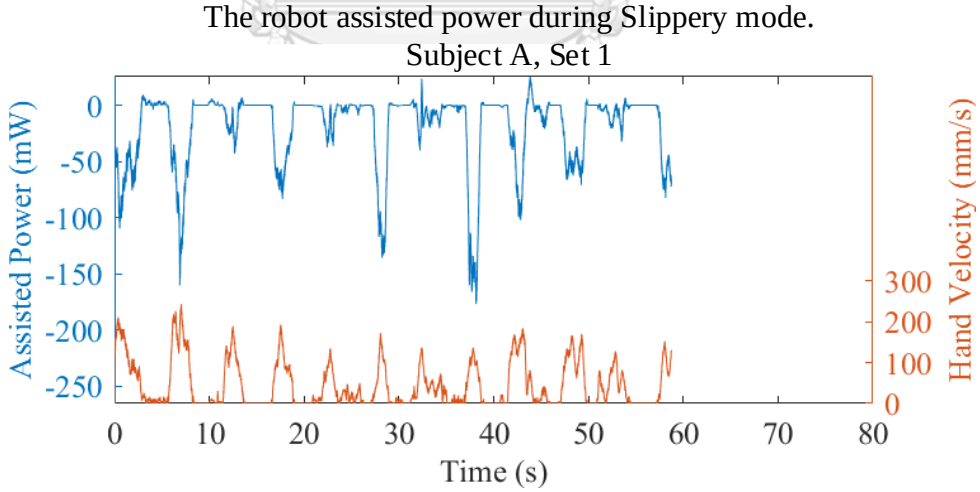

Figure 4.14 Robot-assisted power during slippery mode evaluation.

4.3.4 Results of Force Amplifier Mode.

During the force amplifier mode evaluation of the subject A's first set, the subject's maximum hand velocity exceeds 240 mm/s (Figure 4.15). The total time and moving time is not significantly different from the slippery mode (Table 4.4 and Table 4.5). The energy loss during the task is 243 mJ (Table 4.6), which is significantly less than the slippery mode. In some trajectory, the robot-assisted power is largely positive at acceleration and moving phase. It seems that the force amplifier controller assists the subject in doing the task as designed.

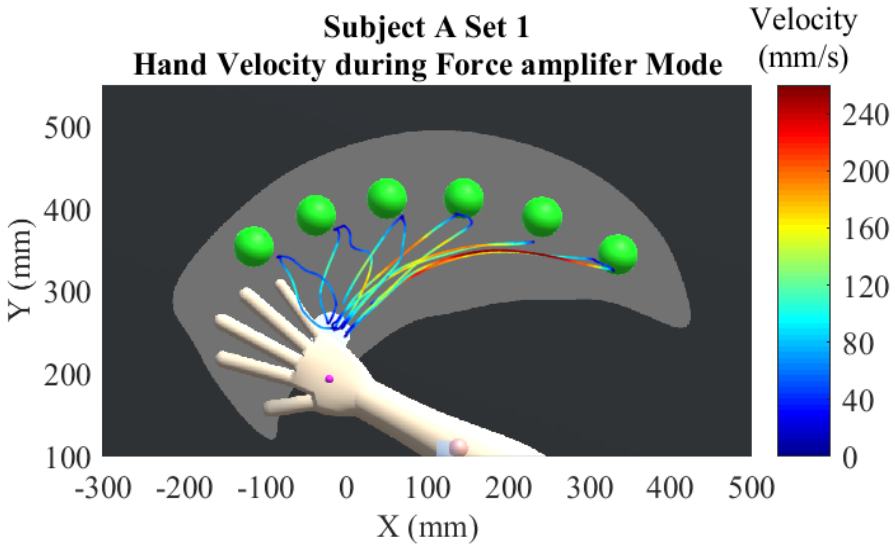

Figure 4.15 Hand velocity during force amplifier mode evaluation.

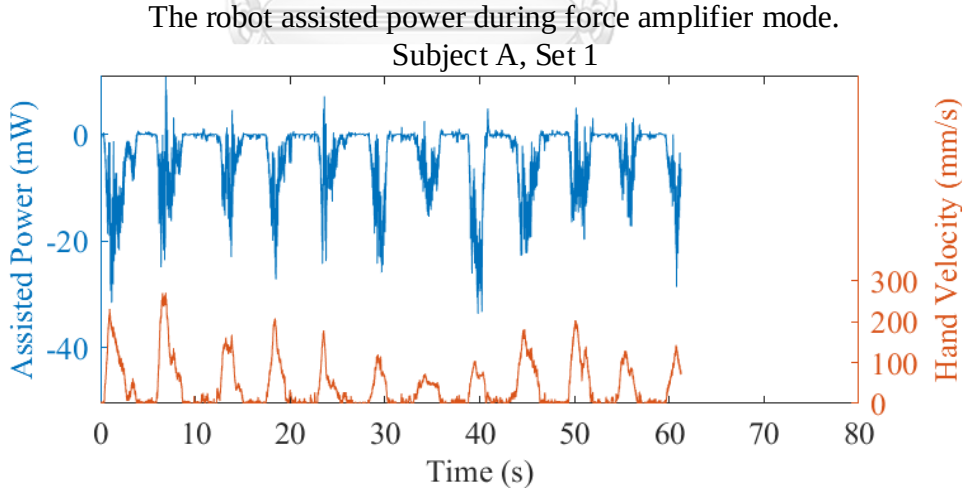

Figure 4.16 Robot-assisted power during force amplifier mode evaluation.

CHAPTER 5
CONCLUSION AND DISCUSSION

5.1 Conclusion

This research presents a 2-DOF upper-limb rehabilitation robot system with a VE. The theoretical backgrounds and literature reviews relate to this research are summarized in Chapter 2. Chapter 3 describe designing of the rehabilitation robot system, which includes the mechanical hardware, electronics hardware, controller software and the Virtual Environment (VE) game. Chapter 4 shows the result of evaluating the rehabilitation robot system with 2 healthy subjects.

The designed rehabilitation robot has been evaluated with 2 healthy subjects, and the results demonstrate effective performance in all of 4 proposed modes.

The passive mode evaluation is to evaluate the position controlling performance. The position error at the end-effector in passive mode is less than 6 mm, and less than 30% maximum driving torque is used.

The power off mode evaluations indicates that the robot has very high backdrivability. The energy loss in the task is less than 2000mJ, while the maximum interaction force is less than 2.5 N.

The slippery mode evaluations indicate that the friction compensator is able to reduce energy loss averagely 27.2%

The force amplifier mode evaluations indicate that the designed force amplifier controller is able to assist the subject motion without knowing the task. The controller assists the motion by reducing interaction force, reducing energy loss and apply assistance force during the motion. The force amplifier is able to reduce energy loss averagely 75.9% from the slippery mode and 82.4% from the power off mode.

5.2 Discussion

From the passive mode evaluations, it was found that there is a static force even the subjects have no intention. The static force seems to bring the subject's arm to certain poses. This means that the subjects need to exert force to hold poses other than the static poses. This static force seems to be very large which may make the subjects not able to do the task if their limbs are weakened. The resistance force from the robot's imperfect backdrivability is very low comparing to this static force. If this static force is compensated, it should be easier to do the tasks.

From the slippery mode, it appears that the robot resists braking intention of the subjects while acceleration resistance is lowered. This is an effect of the robot inertia with very low friction. This effect seems to be decreased by the side effect of the force amplifier controller. This force amplifier minimizes the interaction force between the robot and the user in a horizontal plane and makes the user feel the robot only gives gravity compensation.

The force amplifier mode evaluations show that the controller continuously decreases resistance force but only assist when the subjects do fast acceleration. This assistance energy can be increased by increasing time delay and proportional gain. But increasing time delay will decrease the capability of the controller when the motion is fast (fast acceleration and braking). If the user moves too fast when the time delay is high, the user will feel that the robot is resisting his/her intention. In the end, the controller should be tuned to match the speed capability of the user. Before the evaluations, the subject A tested the force amplifier mode and asked the author to decrease the assistance. The controllers evaluated on the subject A and the subject B are the same.

5.3 Suggestions

In the author's opinion, a patient with weakened upper-limb may need static force compensation more than the force amplifier. The force amplifier controller can be redesigned into a force controller which can be implemented with static force compensation. The static force compensation can be designed by finding a relation between static force and poses.

For this research, an x86 desktop PC and industrial motor driver are used to control the robot. The only reasons for using a large desktop PC are being the fastest way to prove controller concept and it can read the F/T sensor. If the F/T sensor is not needed and controller concepts are done, a custom-made controller, motor driver and power supply can be embedded inside the robot. Doing so will make the system more compact as the only interface out is an Ethernet port for communication with VE. An example of a controller that can control this robot is a controller used in [10], which is capable of 10 kHz sampling rate.

REFERENCES

1. P. Patrizia, M. Giovanni, G. Rosati, and S. Masiero, "Robotic technologies and rehabilitation: New tools for upper-limb therapy and assessment in chronic stroke," BioMed Research International 2013.
2. H.-C. Huang, K.-C. Chung, D.-C. Lai, and S.-F. Sung, "The Impact of Timing and Dose of Rehabilitation Delivery on Functional Recovery of Stroke Patients," J Chin Med Assoc, 2009, vol. 72, pp. 257-264.
3. D. Jack, R. Boian, A. S. Merians, M. Tremaine, G. C. Burdea, S. V. Adamovich, M. Recce, and H. Poizner, "Virtual reality-enhanced stroke rehabilitation," IEEE Transactions on Neural Systems and Rehabilitation Engineering, 2001. vol. 9, no. 3, pp. 308-318.
4. Signe Brunnstrom, "Motor Testing Procedures in Hemiplegia: Based on Sequential Recovery Stages," Physical Therapy, 1966, vol. 46, no. 4, pp. 357-375.
5. P. S. Lum, C. G. Burgar, P. C. Shor, M. Majmundar, and M. Van der Loos, "Robot-assisted movement training compared with conventional therapy techniques for the rehabilitation of upper-limb motor function after stroke," Archives of Physical Medicine and Rehabilitation, 2002, vol. 83, no. 7, pp. 952-959.
6. Y. Mao, X. Jin, G. G. Dutta, J. P. Scholz, and S. K. Agrawal," Human Movement Training With a Cable Driven ARm EXoskeleton (CAREX)," IEEE Transactions on Neural Systems and Rehabilitation Engineering, 2015, vol. 23, no. 1, pp. 84-92.
7. A. Schiele, and F. C. T. van der Helm, "Kinematic Design to Improve Ergonomics in Human Machine Interaction," IEEE Transactions on Neural Systems and Rehabilitation Engineering, 2006, vol.14, no. 4, pp. 456-469.
8. J.C. Perry, J. Rosen, and S. Burns, "Upper-Limb Powered Exoskeleton Design," IEEE/ASME Transactions on Mechatronics, 2007, vol. 12, no. 4, pp. 408-417.
9. www.acefitness.org.
10. N. Angsupasirikul, and R. Chancharoen, "Design of a Backdrivable Triglide Robot," MATEC Web of Conferences, 2015, vol. 26.
11. J.Rosen, M. Brand, M. B. Fuchs, and A. Mircea, "A myosignal-based powered exoskeleton system." IEEE Transactions on Systems, Man, and Cybernetics - Part A: Systems and Humans, 2001, vol. 31, no. 3, pp. 210-222.
12. R.J. Sanchez, J. Liu, S. Rao, et al., "Automating Arm Movement Training Following Severe Stroke: Functional Exercises With Quantitative Feedback in a Gravity-Reduced Environment," IEEE Transactions on Neural Systems and Rehabilitation Engineering, 2006, vol. 14, no. 3, pp. 378-389.

13. S. J. Ball, I.E. Brown, and S.H. Scott, "MEDARM: a rehabilitation robot with 5DOF at the shoulder complex," IEEE/ASME international conference on advanced intelligent mechatronics, 2007.

14. S. J. Ball, I. E. Brown, and S. H. Scott, "A planar 3DOF robotic exoskeleton for rehabilitation and assessment," International Conference of the IEEE Engineering in Medicine and Biology Society, 2007.

15. R. A. R. C. Gopura, K. Kiguchi, and Y. Li, "SUEFUL-7: A 7DOF upper-limb exoskeleton robot with muscle-model-oriented EMG-based control," IEEE/RSJ International Conference on Intelligent Robots and Systems, 2009.

16. M. H. Rahman, T. K. Ouimet, M. Saad, et al. "Control of a powered exoskeleton for elbow, forearm and wrist joint movements," IEEE International Conference on Robotics and Biomimetics. 2011.

17. T. Lenzi, N. Vitiello, S. M. M. De Rossi, et al. "NEUROExos: A variable impedance powered elbow exoskeleton," IEEE International Conference on Robotics and Automation, 2011, pp. 1419-1426.

18. N. Vitiello, T. Lenzi, S. Roccella, et al., "NEUROExos: A Powered Elbow Exoskeleton for Physical Rehabilitation," IEEE Transactions on Robotics, 2013. vol. 29, no. 1, pp. 220-235.

19. Y. Mao, and S. K. Agrawal, "Design of a Cable-Driven Arm Exoskeleton (CAREX) for Neural Rehabilitation," IEEE Transactions on Robotics, 2012, vol. 28, no. 4, pp. 922-931.

20. A. J. Westerveld, B. J. Aalderink, W. Hagedoorn, et al., "A Damper Driven Robotic End-Point Manipulator for Functional Rehabilitation Exercises After Stroke," IEEE Transactions on Biomedical Engineering, 2014, vol. 61, no. 10, pp. 2646-2654.

21. N. Angsupasirikul, , and R. Chancharoen. "An end-effector arm rehabilitation robot with VE," IEEE International Conference on Rehabilitation Robotics (ICORR), 2015.

22. A. Sutapun, and V. Sangveraphunsiri, "A Novel Design and Implementation of a 4-DOF Upper Limb Exoskeleton for Stroke Rehabilitation with Active Assistive Control Strategy," Engineering Journal, 2017, vol. 21, no. 7, pp. 275-291.

23. T. Lenzi, S. M. M. De Rossi, N. Vitiello, and M. C. Carrozza, "Proportional EMG control for upper-limb powered exoskeletons," International Conference of the IEEE Engineering in Medicine and Biology Society, 2011.

24. K. Kiguchi, and Y. Hayashi, "An EMG-Based Control for an Upper-Limb Power-Assist Exoskeleton Robot," IEEE Transactions on Systems, Man, and Cybernetics, Part B (Cybernetics), 2012, vol. 42, no.4, pp. 1064-1071.

25. Z. Li, B. Wang, F. Sun, et al., "sEMG-Based Joint Force Control for an Upper-Limb Power-Assist Exoskeleton Robot," IEEE Journal of Biomedical and Health Informatics, 2014, vol. 18, no. 3, pp. 1043-1050.

26. W. Ye, Z. Li, and C.Y. Su, "Development and human-like control of an upper limb rehabilitation exoskeleton using sEMG bio-feedback," IEEE International Conference on Mechatronics and Automation, 2012.

27. M. Steinisch, M.G. Tana, and S. Comani, "A Post-Stroke Rehabilitation System Integrating Robotics, VR and High-Resolution EEG Imaging," IEEE Transactions on Neural Systems and Rehabilitation Engineering, 2013, vol. 21, no. 5, pp. 849-859.

28. M.A. Padilla-Castañeda, E. Sotgiu, A. Frisoli, et al., "A virtual reality system for robotic-assisted orthopedic rehabilitation of forearm and elbow fractures," IEEE/RSJ International Conference on Intelligent Robots and Systems, 2013.

APPENDIX

VITA

Natthapong Angsupasirikul was born on 23th January 1992. He received a bachelor's degree in mechanical engineering from Chulalongkorn University in 2014. With interesting in developing robotic system, he continued studying Master of Mechanical Engineering program of this university.